# Multiresolution Models of Financial Time Series

by

Paul Stephan Mashikian

S.B., Massachusetts Institute of Technology, 1996
S.B., Massachusetts Institute of Technology, 1996

Submitted to the Department of Electrical Engineering and Computer Science
in partial fulfillment of the requirements for the degree of

Master of Engineering in Electrical Engineering and Computer Science

at the

MASSACHUSETTS INSTITUTE OF TECHNOLOGY

June 1997



Author .....
Department of Electrical Engineering and Computer Science
May 23, 1997

Certified by .....
Andrew W. Lo
Harris & Harris Group Professor
Thesis Supervisor

Accepted by .....
Arthur C. Smith
Chairman, Department Committee on Graduate Theses

# Multiresolution Models of Financial Time Series

by

Paul Stephan Mashikian

Submitted to the Department of Electrical Engineering and Computer Science
on May 23, 1997, in partial fulfillment of the
requirements for the degree of
Master of Engineering in Electrical Engineering and Computer Science

## Abstract

Multiresolution stochastic models on dyadic trees are presented and used to model financial time series. The wavelet transform, the basis for decomposing signals along both scale and time, is investigated and employed in the study of stock market data. The statistics of the wavelet coefficients of stock and foreign exchange returns are used to guide the multiscale modeling process. An overview of different multiscale autoregressive models is presented accompanied by corresponding parameter estimation algorithms. The multiresolution model parameters are estimated for three indices, ten individual stocks, and a foreign exchange rate. The robust nature of these models offers potential for further development in the scope of finance.

Thesis Supervisor: Andrew W. Lo
Title: Harris & Harris Group Professor

# Acknowledgments

I would like to express my appreciation to my thesis supervisor, Andrew Lo, for his guidance, advice and faith in me.

I owe a great deal to other members of the faculty as well. Professor Al Drake was a constant source of inspiration during my term as a teaching assistant under him. He furthermore is one of the most caring people that I know.

I also would like to thank a number of the faculty who did not directly contribute to this thesis, however, they both inspired and educated me with their teaching. I thank professors Gilbert Strang, Robert Gallagher, and Al Oppenheim.

I sincerely thank my academic advisor, Professor Paul Gray, for his support, kindness, and direction. I especially appreciate his help in refocusing my energy on education after I lost some of my motivation.

I thank Walter Sun, Marc Burock, Iyad Obeid, and Cynara Wu, fellow teaching assistants, who constantly listened to my complaints about how much work I had, and offered motivational support.

I thank all of my brothers at the Delta Upsilon Fraternity with whom I shared what will doubtless be some of the best times in my life. I especially thank David Brandenburger, Andy Scott, Morio Alexander, and Samuel Pearlman.

I am deeply grateful to my parents, Matthew and Margarethe Mashikian, who have supported me through everything, both good and bad. I thank my father especially for understanding and whole-heartedly supporting my choice to work in finance rather than electrical engineering. I lastly thank my sister Sonia for always being so supportive.

# Contents

# List of Figures

# List of Tables

# Chapter 1

# Introduction

## 1.1 Motivation for Research

Financial markets serve as an arena for people to make bold decisions about securities without fully understanding everything that will affect the price of the security. In short, securities have large random components in their pricing. Since no one has a crystal ball to tell what the future price of a stock will be, people try to model price behavior. Some people favor regression models that take economic factors such as inflation and unemployment into account, while others treat the price of a stock simply as a time series. It is the latter case that is the interest of this thesis.

Stochastic time series models have been employed as a means of modeling stock prices for almost a century. The early models characterized stock prices as random walks. These models evolved in the late 1950s into geometric Brownian motion, or diffusion models. Lately there has been interest in similar diffusion models that also exhibit discontinuous jump components. All of these models are examples of processes that evolve in time. Such standard time series models have been around for a relatively long time. A new development in mathematics has been the study of stochastic processes which are generated on trees. These processes evolve in scale as well as time.

The goal of this thesis is to examine the ability of multiscale stochastic processes to explain both the short- and long-term variations in stock prices. Such a multiscale

model essentially treats data as the combination of data at different resolutions which are related to one another. This approach seems natural considering the different scales at which market microstructure and macrostructure affect stock prices.

## 1.2 Research Problem Statement

This thesis presents a family of multiresolution stochastic models for security prices. This family of models is grounded in wavelet theory which provides a decomposition of signals according to scale. We attempt to model the coefficients of this decomposition, the so-called wavelet coefficients, as being the output of an all-pole (autoregressive) filter driven by scale-varying white noise.

Using the discrete wavelet transform (DWT) we study the wavelet and scaling coefficients of stock and foreign exchange time series in a multiresolution framework. We use these multiresolution analyses to steer our multiscale models for financial data. Minimum mean square error estimation is employed to estimate the parameters of our models for each stock and foreign exchange rate.

## 1.3 Background and Literature Review

### 1.3.1 Wavelets

The name wavelet means little wave, which is an appropriate way to describe what a wavelet actually is, a little, localized wave. These little waves have gained rather big attention in recent years due to their ability to analyze data according to scale as well as efficiently handle choppy data. Wavelet analysis has evolved from a very restricted field into a growing and coherent one. The current trend is to establish the use of wavelets as a staple in signal processing, similar to the current status of Fourier analysis.

The study of wavelets began in the early 1900s with the work of Alfred Haar [23] in 1910. Haar generated a basis with compact support which consisted of simple piecewise constant sections. The applications of Haar's wavelet were very limited due

to it not being continuously differentiable. In the 1930s, several people investigated the use of scale-varying basis functions in research. Paul Levy, a physicist showed that Haar's basis function was superior to Fourier analysis for the study of Brownian motion. Between 1960 and 1980, several efforts were made to break up functional spaces into a set of simplest elements and later reconstruct the spaces. This work led to various efforts in engineering, physics, and mathematics to represent signals according to scale [22].

In 1985, Stephane Mallat [29] sparked the modern surge in wavelet research by studying the role of the pyramid algorithm in multiresolution analysis and its connections to orthonormal wavelet bases. Shortly thereafter, Yves Meyer [30] constructed a set of non-trivial wavelets that were continuously differentiable. Despite these advances, it was Ingrid Daubechies [13] who revolutionized the study of wavelets by introducing a family of smooth, orthonormal wavelets. In the 1990s, Daubechies [14] again stepped to the forefront by writing a key book in 1992. In the subsequent years, the theories developed in engineering, physics and mathematics have converged to produce a unified and important topic in mathematics. For this unified representation of wavelets, one can refer to Strang [36] (1996).

### 1.3.2 Multiscale Signal Processing

Multiscale or multirate signal processing is a topic that was originally developed independently of wavelet theory. In 1983, Crochiere and Rabiner [12] published a book on multirate digital signal processing. Also in 1983, Burt and Adelson [8] used multiresolution methods in computer vision problems. As mentioned in Section 1.3.1, Stephane Mallat [28] combined the idea of multiresolution analysis with the study of wavelets.

From the late 1980s through 1993, a combined effort between the Massachusetts Institute of Technology (MIT) and the Institut de Recherche en Informatique en Systemes Aleatoires (IRISA) [20, 10, 6, 9] produced a framework for encorporating a structured system theory for multiscale processes defined on trees. Golden [20] (1991) develops theory regarding the construction of quadrature mirror filterS (qmf) for per-

fect reconstruction in filter banks. Golden's work concentrates on the decorrelation of wavelet coefficients due to choice of qmf pair. Chou [10] (1991) develops an approach to modeling multiscale processes on both trees and lattices. Basserville, et al. [6] (1992) present a unified theory of multiresolution stochastic modeling and optimal multiscale signal processing. In 1993, Chou, et al. [9] complete the research with a presentation of their multiresolution stochastic models as well as optimal signal processing algorithms for smoothing and fusion of data is such a framework. Following the lead of MIT and IRISA, Dijkerman and Mazumdar [17] (1994) look at multiresolution stochastic models which are similar to those proposed above. As opposed to the MIT and IRISA work, Dijkerman and Mazumdar present a nonstationary multiresolution model.

More recent books on multiscale signal processing have been published as well. The recent treatments of this topic are [2, 11, 19, 27, 39].

### 1.3.3 Wavelet Applications to Time Series

Thoughout the evolution of wavelets, a great deal of attention has been paid to the analysis of time series. In fact, the research of Goupillaud, et al. [21] (1985) on seismic time series was one of the original applications of wavelets. Davis, et al. [15] (1994) presents the usefulness of wavelet analysis with nonstationary and intermittent signals. Another geophysical time series application can be found in Bolton, et al. [7] (1995), which performs a wavelet analysis for time series that exhibit time-dependencies in the periods of their dominant cycles. Moreau et al. [31] (1996), uses the wavelet transform for filtering and denoising of time series. Further geophysical applications deal with the scale analysis of time series, such as Lindsay, et al. [26] (1996).

Another important time series topic for wavelets has been the study of fractional Brownian motion (fBm). Fractional Brownian motion represents a nonstationary random process with stationary increments which is commonly used for modeling long-range dependent data. Wornell [38] (1993), Dijkerman and Mazumbar [16] (1994) and Abry, et al. [1] (1995) developed the theory of the correlation of wavelet coefficients

for fBm. This case is special as the discrete wavelet transform almost completely decorrelates these wavelet coefficients. In addition, they present methods for estimating the Hurst exponent using wavelet techniques. Jones, et al. [24] (1996) present yet another method for estimating the Hurst exponent using wavelet packets. Finally, Kaplan and Kuo [25] (1996) develop the notion of extended self-similarity or asymptotic fractional Brownian motion (afBm) which encorporates short-term correlations. They base their parameter estimation for this model on the Haar wavelet transform of their data.

In a closely related field, wavelets are often used in studying long-memory processes. Percival and Guttorp [32] (1994) use the Haar wavelet to find the Allan variance of long-memory processes. Arnedo et al. [5] (1995) use the wavelet transform to characterize long-range dependencies in DNA sequences. The effectiveness of the wavelet transform for this task is due to its ability to handle patchy and choppy data.

### 1.3.4 Wavelets in Financial Time Series

Ramsey, et al. [33] (1994) present an analysis of S&P 500 data using the wavelet transform. They use the transform as a means of looking for self-similarity and structure within different scales. This article is definitely a first step in investigating financial data and is essentially an extension of wavelet analysis used on turbulence data. Ramsey found evidence of quasi-periodicity in the stock index that led to the conclusion that the data was more than geometric Brownian motion.

Arino [3] (1995) and Arino and Vidakovic [4] (1995) present methods in which the wavelet scalogram can be used as a tool in forecasting seasonal economic time series. The basic idea is that time series are composed of components at different scales. By using the wavelet scalogram, one can separate the signal into different energy bands to be forecasted separately. The wavelet transform is also used to denoise the signal via wavelet shrinkage. The separate denoised scale bands are then used to produce a forecast using the Box-Jenkins approach. In this method, however, Arino uses a forecast in the beginning to extend the signal to avoid edge effects. This signal

extension, while necessary, introduces a bias into the forecast.

## 1.4 Outline

Chapter 2 presents the requisite theory of multirate signal processing. This presentation emphasizes the importance of the wavelet transform in our modeling. The theory of multiresolution analysis and wavelet scalograms is also described.

Chapter 3 presents processes on dyadic trees, in general, and those generated from multiscale autoregressive models in particular. Design considerations and parameter estimation algorithms are presented for these models.

Chapter 4 presents the multiresolution analysis of both stock and foreign exchange returns. The first section describes the data and its source. The second section provides both qualitative and quantitative analysis of our study.

Chapter 5 presents the results of the empirical modeling. Parameter estimation is performed for our multiscale models.

Chapter 6 summarizes the important results of this thesis and discusses the implications of multiscale modeling in finance.

# Chapter 2

# Multirate Signal Processing

## 2.1 The Wavelet Transform

### 2.1.1 Continuous Wavelet Transform

In a general sense, the wavelet transformation of a signal $x(t)$,

$$x(t) \Longleftrightarrow X_\nu^\mu$$

is defined by projections of $x(t)$ onto translations and dilations of a "Mother" wavelet $\psi(t)$, such that [39]

$$X_\nu^\mu = \int_{-\infty}^{\infty} x(t)\psi_\nu^\mu(t)dt \tag{2.1}$$

where

$$\psi_\nu^\mu(t) = |\mu|^{-\frac{1}{2}}\psi(\frac{t-\nu}{\mu}).$$

In this continuous representation, $\mu$ and $\nu$ are dilation and translation parameters, respectively. They can take on any value, except for the condition that $\mu \neq 0$. In order to be an invertible transform, we require that $\psi(t)$ satisfies the admissibility condition:

$$\int_{-\infty}^{\infty} |\Psi(\omega)|^2|\omega|^{-1}d\omega = C_\psi < \infty, \tag{2.2}$$

where $\Psi(\omega)$ is the Fourier transform of $\psi(t)$. For a wavelet that satifies $C_\psi < \infty$, we can reconstruct $x(t)$ according to

$$x(t) = \frac{1}{C_\psi}\int_{-\infty}^{\infty}\int_{-\infty}^{\infty} X_\nu^\mu \psi_\nu^\mu(t)\mu^{-2}d\mu d\nu. \tag{2.3}$$

In certain cases, it is possible to reconstruct $x(t)$ from the $X_\nu^\mu$ on a hyperbolic lattice with

$$\mu = a^{-m}$$

$$\nu = nba^{-m}$$

for any $n, m$ which represent the new translation and dilation parameters, respectively. In such a representation, $a$ and $b$ are the increments of dilation and translation. The dyadic wavelet bases created by setting $a = 2$ and $b = 1$ have become a major focus in wavelet research.

### 2.1.2 Discrete Wavelet Transform

When dealing with orthonormal bases, in the dyadic framework mentioned above, we represent the orthonormal wavelet transformation of a signal $x(t)$,

$$x(t) \Longleftrightarrow x_n^m.$$

From the theory generated for the continuous transform, we define

$$x_n^m = \int_{-\infty}^{\infty} x(t)\psi_n^m(t)dt, \tag{2.4}$$

where

$$\psi_n^m(t) = 2^{\frac{m}{2}}\psi(2^m t - n). \tag{2.5}$$

The process of breaking down the signal $x(t)$ with our wavelet basis is referred to as analysis. The counterpart of analysis is synthesis. The goal of synthesis is to construct the signal $x(t)$ using our wavelet basis. The synthesis equation for orthonormal

wavelet transforms is defined as

$$x(t) = \sum_m \sum_n x_n^m \psi_n^m(t). \tag{2.6}$$

The basis function $\psi(t)$ has been referred to as the "Mother" wavelet, because all $\psi_n^m(t)$ are derived from $\psi(t)$. In a similar fashion, we talk about a so-called scaling function, or "Father" wavelet, $\phi(t)$. This scaling function should satisfy the *dilation equation* [36]

$$\phi(t) = \sum_n h(n)\phi(2t - n). \tag{2.7}$$

The wavelet $\psi(t)$ is derived from $\phi(t)$ according to

$$\psi(t) = \sum_n g(n)\phi(2t - k). \tag{2.8}$$

The $h(n)$ and $g(n)$ correspond to a lowpass and highpass filter respectively. The two filters form a Quadrature Mirror Filter (QMF) pair. For orthonormal wavelets, we have

$$g(n) = (-1)^n h(N - n),$$

where $N + 1$ is the length of the lowpass filter $h(n)$.

We can alternatively derive the QMF pair from $\psi(t)$ and $\phi(t)$ via

$$h(n) = \int_{-\infty}^{\infty} \phi_n^1(t)\phi_0^0(t)dt \tag{2.9}$$

$$g(n) = \int_{-\infty}^{\infty} \phi_n^1(t)\psi_0^0(t)dt \tag{2.10}$$

Further discussion of how the QMF pair is selected will be presented in a later section.

## 2.2 Multiresolution Analysis

When discussing the wavelet transform, we projected our signal $x(t)$ onto basis functions $\psi_n^m(t)$ to get wavelet coefficients $x_n^m$. We define multiresolution analysis as the decomposition of signal space $\mathbf{V}$ into its subspaces $V_m$, the signal approximation at

resolution $m$. We further require [34]:

1. $V_m \subset V_{m+1}$ for all integers $m$
2. $\cup V_m = L^2$
3. $\cap V_m = 0$.

Since the $V_m$ are nested subspaces, we can represent the approximation of $x(t)$ on the subspace $V_{m+1}$ in terms of $V_m$ and its orthogonal complement $W_m$. We thus realize

$$V_{m+1} = V_m \bigoplus W_m,$$

where $V_m$ and $W_m$ are the projections of $x(t)$ onto the space spanned by the scaling and wavelet basis functions $\phi_n^m(t)$ and $\psi_n^m(t)$, respectively. One can now see the connection between multiresolution analysis and wavelets. Multiresolution analysis deals with the approximation of a signal at different resolutions, while wavelet analysis deals with the differences between approximations at successive resolutions.

### 2.2.1 Approximations of Signals at Varying Resolutions

As previously stated, the approximation of $x(t)$ in the subspace $V_m$ is attained by projecting $x(t)$ onto $\phi_n^m(t)$, where we define

$$\phi_n^m(t) = 2^{\frac{m}{2}} \phi(2^m t - n). \tag{2.11}$$

We therefore represent the approximation at resolution $m$ as

$$\hat{x}_m(t) = \sum_n a_n^m \phi_n^m(t) \tag{2.12}$$

where $a_n^m$ represent the approximation coefficients at the resolution $m$ and translation $n$. We calculate the approximation coefficients via

$$a_n^m = \int_{-\infty}^{\infty} x(t) \phi_n^m(t) dt. \tag{2.13}$$

Due to the nested nature of our subspaces, we could alternatively represent our approximation at resolution $m$ using wavelets:

$$\hat{x}_m(t) = \sum_{l=-\infty}^{m-1} \sum_n x_n^m \psi_n^l(t). \tag{2.14}$$

In multiresolution analysis, we look at the approximation coefficients, $a_n^m$, as containing the coarse information of $x(t)$, while the wavelet coefficients, $x_n^m$, represent the detailed information. Carrying this coarse versus detail argument further, we refer again to our QMF pair $h(n)$ and $g(n)$. Since a lowpass filter picks out coarse structure, while a highpass filter picks out details, we have:

$$a_k^m = \sum_n h(n-2k) a_n^{m+1} \tag{2.15}$$

$$x_k^m = \sum_n g(n-2k) a_n^{m+1}. \tag{2.16}$$

Further discussions of multiresolution and wavelet approximations are discussed in [29, 36].

### 2.2.2 Scalograms

The idea behind scalograms is not directly related to the approximation concept of multiresolution analysis, however, it also yields information about the signal $x(t)$ at various resolutions. A wavelet scalogram does in scale what a periodogram does in frequency. Namely, a scalogram represents the decomposition of the energy of a signal at different resolutions. We define the scalogram quantities as

$$E_m = \frac{1}{N_m} \sum_n (x_n^m)^2 \tag{2.17}$$

where $N_m$ is the number of wavelet coefficients at the $m$th resolution level of the signal $x(t)$ [4].

For a signal with length $N$, where $N = 2^j$ for $j$ any positive integer, we represent

our scalogram vector $\mathbf{E}$ by

$$\mathbf{E} = [(\mathbf{a_n^m})^2, \mathbf{E_0}, \mathbf{E_1}, \mathbf{E_2}, \ldots, \mathbf{E_{j-1}}]. \tag{2.18}$$

By plotting the $j$ values of the vector $\mathbf{E}$ we can visually see the distribution of power in the signal according to scale. We will see later how understanding this progression of wavelet coefficient variances will be useful in the modelling of multiscale processes.

## 2.3 QMF Filter Design

In the previous section, we concentrated on the wavelet and scaling functions, $\psi(t)$ and $\phi(t)$, respectively. In this section, the focus shifts to the QMF pair $h(n)$ and $g(n)$.

### 2.3.1 Perfect Reconstruction Condition

Let us start out by stating the perfect reconstruction (PR) condition. The idea of perfect reconstruction for QMF filters is that an analysis and synthesis step exist, such that we can inverse transform our transformed signal to get back the original signal. Formally, the perfect reconstruction condition is stated as

$$\delta_{n,p} = \sum_k (h(2k-n)h(2k-p) + g(2k-n)g(2k-p)). \tag{2.19}$$

Derivation of this condition is beyond the scope of this thesis, however, there exists extensive literature regarding regarding QMF filter design as well as derivation of the PR condition. I refer the reader to [36, 20, 37]. What is important from the PR condition, is that it can be solved by choosing

$$g(n) = (-1)^n h(N-n).$$

### 2.3.2 Orthogonality Condition

The orthogonality condition states that we want our analysis filter to be inverted by its transpose. By ensuring orthogonality, we generate wavelets that are orthogonal to all of their dilates and translates. This condition is important because it allows us to do an orthonormal decomposition of signals via the wavelet transform. Extensive discussion of this condition is covered in [36].

### 2.3.3 Accuracy of Approximation Condition

The approximation condition has to do with the number of vanishing moments in the lowpass filter $h(n)$. A vanishing moment is equivalent to having a *zero* at $\pi$ in the frequency response of the filter. This can be stated as

$$H(z) = (\frac{1+z^{-1}}{2})^p Q(z) \tag{2.20}$$

where $H(z)$ is the $z$-transform of $h(n)$ and $Q(z)$ is the $z$-transform of another filter with no zeros at $\pi$. The higher the order of $p$, the greater the decorrelation of wavelet coefficients, $x_n^m$. By having uncorrelated or nearly uncorrelated coefficients, we can achieve a Karhoenen-Loeve-like transformation which allows us to achieve excellent approximations of $x(t)$ with the use of only a few of the wavelet coefficients. Additional methods of creating QMFs that optimize the decorrelative effects for given processes are discussed in [20]. An important note is that the counting of vanishing moments is very similar to the idea of regularity that is often discussed in the context of wavelets. The implications of the two concepts are essentially identical.

## 2.4 Discrete-Time and Finite-Length Sequences

In the discussion of wavelet transforms above, it is assumed that the $x(t)$ is a continuous signal. Even in the discrete wavelet transform, the discrete represents the dilation and translation increments. In addition, it is assumed that $x(t)$ has infinite length. When these two conditions on $x(t)$ are violated, the theory of wavelets is not

as precise and leaves several choices to make in how to use the data.

### 2.4.1 Discrete-Time Sequences

Since the advent of digital computers, it has been convenient to deal with discrete-time sequences. Such discrete series usually come from the sampling of continuous-time processes. In the case of financial data, we concentrate on discrete time series data, $x[n]$. These series either represent regularly sampled points of a continuous price process, such as daily closing prices, or irregularly points, such as tick-by-tick trading data. The question of interest is whether we should use these samples as the approximation coefficients, $a_n^m$, at the finest level or whether we should make an adjustment to account for the fact that they are samples. The problem involved stems from the fact that

$$\hat{x}_m(t) = \sum_n x[n]\phi_n^m(t)$$

evaluated at the sample times does not yield the $x[n]$. In other words, the continuous-time process corresponding to using $x[n]$ as approximation coefficients is different from the process that yields $x[n]$ as samples.

Although Strang [36] refers to this practice as a "wavelet crime", he concedes that it is often commited out of convenience. Several methods have been proposed to account for this problem. Rioul and Duhamel [35] the use of analog-to-digital converters which can find the approximation coefficients, which correspond to a make-believe process, directly from the samples $x[n]$. Donoho [18] suggested the use of an interpolating wavelet transform. Rao and Indukumar [34] suggested a third method which involves first interpolating the sequence $x[n]$ using the sinc function to produce $x(t)$:

$$x(t) = \sum_n x[n]\frac{sin(\pi(t-n))}{\pi(t-n)}. \tag{2.21}$$

This method is further refined by combining it with the first approximation as defined by the discrete wavelet transform. The result is consistent approximation coefficients which can be used to produce all other scaling coefficients at coarser resolutions.

### 2.4.2 Finite-Length Sequences

The goal of this section is to discuss the consequences of using the discrete wavelet transform on a finite length sequence. The dyadic nature of the discrete wavelet transform means that there are $2^m$ wavelet coefficients at the $m$th resolution. If a signal with finite length, $M$, is linearly convolved with a filter with length $N$, then the result is a sequence with length $M + N - 1$. We can see that this linear convolution introduces a contradiction with our idea of a dydic discrete wavelet transform, in that the number of coefficients at adjacent scales will not be multiples of two of one another.

Various schemes have been developed to maintain the dydic nature of the discrete wavelet transform. Some of these methods include circular convolution, zero-padding, symmetric extension and boundary filters [36]. The general idea with all of these methods is that we will suffer from some distortion at the edges of our signal. Depending on the nature of the use of the discrete wavelet transform, we will use an appropriate solution for finite data length. In the case of modeling, edge effects can be noticed, however, are not of significant concern. It is, however, important not to forget that they exist, as these edge effects can hinder any attempt to use these models for prediction. A further discussion of the many practical issues regarding finite-length sequences can be found in Strang [36] and Golden [20].

# Chapter 3

# Multiscale Stochastic Models

## 3.1 Introduction

In Chapter 2 we discussed the wavelet transform as a means of both analyzing and synthesizing signals. In the analysis case, we use a set of quadrature mirror filters to decompose a signal according to scale and translation. This decomposition can be looked at either as sets of approximation coefficients or as the approximation coefficients at a base scale and the wavelet coefficients for all finer scales. In the latter framework, we discussed how we select a "mother" wavelet with sufficient vanishing moments in order to better approximate the signal with fewer coefficients. Hand-in-hand with this concept is the concept of decorrelating the wavelet coefficients both across a given scale as well as between different scales. Furthermore, when we use an orthogonal "mother" wavelet, our decomposition yields coefficients for an orthogonal expansion.

While the analysis side of the wavelet transform proves very useful in looking at data, the synthesis side is vital to the understanding of multiscale or multiresolution modeling of data. Under the assumption that the wavelet coefficients of a stochastic process represent an almost uncorrelated random process, we can generate such coefficients and use the wavelet transform to synthesize the corresponding multiscale stochastic process. It is the notion that we can dynamically model these wavelet coefficients with regard to their statistics, e.g., mean, variance, and correlation both

within and across scale, that is the backbone of multiscale modeling.

Before attempting to describe our multiscale models, we first must develop a language with which to represent our models. In normal signal processing or statistics applications, we talk about stationary and nonstationary signals. For either type of signal, common practice is to model the correlation between any two points $x(t)$ and $x(s)$. The autocorrelation function in general is referred to as

$$R(t,s) = E[x(t), x(s)], \tag{3.1}$$

where $E[]$ represents the expectation operator. For the case of stationary signals, $R(t,s) = R(t-s)$ due to the shift-invariance implicit in stationarity. As a result of this common representation of stochastic processes, the time coefficient is usually the only parameter of interest. Again, in the special case of stationary signals, we are only interested in lag or distance, $t-s$. In the case of multiscale stochastic processes, we have an analogous need to represent distance. The idea of distance in a process on a tree is, however, quite a different matter.

## 3.2 Processes on Dyadic Trees

A dyadic tree is a tree that has a branching factor of two. In other words, each node has one "parent" node and two "children". In such a representation, we can refer to a node by its position on the tree in terms of scale and shift, $m$ and $n$ respectively. According to this description, each scale $m$ in the dyadic tree has $2^m$ possible shift positions, $n$. As discussed above, representation of processes requires a notion of distance or lag. For normal time series, this distance is usually $|t-s|$. For dyadic trees, we define the distance from any nodes $t$ to $s$, $d(t,s)$, as the number of branches which must be traversed in order to get from node $t$ to $s$.

In ordinary time series study, a shift is either forward or backward. In general, all such shifts can be referred to in terms of the delay operator, $z^{-1}$. Additionally, a forward shift, $z$ is defined, such that $z$ cancels out $z^{-1}$. In the case of dyadic trees,

a forward shift is significantly different from a backward shift. The reason is that a backward shift goes from a "child" to the "parent". A forward shift, however, can go either to the "child" on the left or on the right. It is for this reason, that the forward shift operators on a dyadic tree, $\alpha$ and $\beta$, for forward left and right shifts, respectively are defined as separate operators. The backward shift operator is defined as $\bar{\gamma}$. Another operator that we define is the interchange operator, $\delta$. The interchange operator moves from a node to its "sibling" node. In other words, if node $t$ has "children" $a$ and $b$, then the interchange operator moves you from $a$ to $b$ and vice versa [6]. The final operator is the identity operator 0. We also use the notation $(t \wedge s)$ to denote the node at which $t$ and $s$ have a common parent. $(8 \wedge 10) = 1$ in Figure 3-1.

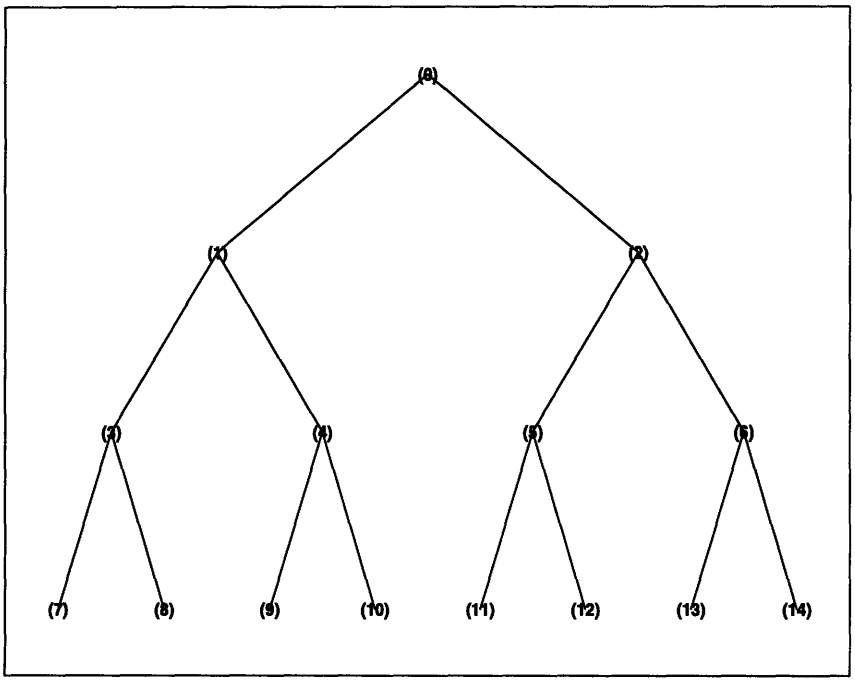


Figure 3-1: Dyadic Tree with 3 Levels

An important concept for processes on trees is the idea of distance. On a tree, distance is specified by the number of branches which must be traversed to get from one node to another. Figure 3-1 shows an example of a few branches of a dyadic tree. The nodes on this tree are labeled from 0 to 14. From our notation above, we can

see that $\delta 8 = 7$. Furthermore, we see that to get from 8 to 7, we follow a branch up to $\bar{\gamma} 8 = 3$ and then go to 7. Based on the need to traverse two branches to get from 8 to 7, we define $d(8,7) = d(7,8) = 2$. In terms of notation described above, we can also denote

$$d(t,s) = \bar{d}(t, t \wedge s) + \bar{d}(s, t \wedge s), \tag{3.2}$$

where $\bar{d}$ describes distance in a purely unidirectional fashion, i.e., the number of steps between the two nodes in an ascending fashion.

### 3.2.1 Stationary Processes

A stochastic process is said to be stationary if its correlation function is invariant to translation. In terms of our notion of distance, this means that $r(t,s) = r(d(t,s))$, where $r$ is the autocorrelation function. This concept of stationarity implies that the correlation between node 7 and node 8, $r(7,8)$, in Figure 3-1 is the same as $r(8,1)$.

Another important concept is the notion of causality. Causality for a process on a dyadic tree is the idea that the values of the wavelet coefficients at one scale are a function only of coefficients at that scale and coarser scales. A complete discussion of stationary, isotropic and causal processes on trees is presented in Basseville, et al. [6].

## 3.3 Stochastic Models

For the purpose of this thesis, we will focus on three general models for our multiscale autoregressive (AR) processes. We will refer to these processes as the 2- and 3-parameter stationary multiscale AR(1) models and the 3-parameter nonstationary AR(2) model. The first two models, suggested in Chou [10], are first order autoregressive, however, the 3-parameter model is driven by white-noise with scale-dependent variance. The 2-parameter model is given by:

$$x_t = a x_{\bar{\gamma} t} + b w_t, \tag{3.3}$$

where $a, b$ are not dependent on scale, $x_t$ represents the wavelet coefficient at node $t$, and $w_t$ is zero-mean, unit variance white Gaussian noise. The 3-parameter model is given by:

$$x_t = a x_{\bar{\gamma}t} + 2^{-\frac{\lambda m}{2}} b w_t, \tag{3.4}$$

where $a$, $b$ and $w_t$ are as above, and $\lambda$ makes the white-noise process's variance scale-dependent. Therefore, we see that we parameterize the 2- and 3-parameter multiscale AR models with $\Theta_2 = (a, b)$ and $\Theta_3 = (a, b, \lambda)$, respectively [10].

Dijkerman and Mazumdar [17] suggest a nonstationary model that incorporates more coefficients on both the same scale and on the parent scale. This sort of model, while nonstationary according to the notion of Section 3.2.1, can be used to encorporate a stiffer notion of causality that covers both time and scale. As mentioned above, our notion of causality is currently one of scale alone. This model, which we will designate as our nonstationary 3-parameter AR(2) model, is given by:

$$x[m, n] = a_1 x[m, n-1] + a_2 x[m-1, [\frac{n}{2}]] + b w[m, n] \tag{3.5}$$

where $[\frac{n}{2}]$ denotes the integer part of $\frac{n}{2}$. Furthermore, $w[m, n]$ is zero-mean, unit-variance white Gaussian noise. The parameter vector for this model is $\Theta_{3n} = (a_1, a_2, b)$.

Other models have been presented in the literature. Basseville, et al. [6] suggests multiscale AR models of higher order. One can see that an autoregressive model of order two on a tree grows from two parameters to four $(a_{\bar{\gamma}}, a_{\delta}, a_{\bar{\gamma}^2}, b)$. The geometric growth of parameters creates troubles and thus Basseville suggest using the reflection coefficients of a lattice filter rather than the $a$'s.

In an even more complicated sense, Chou [10], describes the theory to use models whose parameters ($a$'s,$b$'s) are vectors rather than scalars. Such models could even further allow scale dependencies.

Before discussing the method of parameter estimation, it is important to visualize what sample paths of these processes look like.

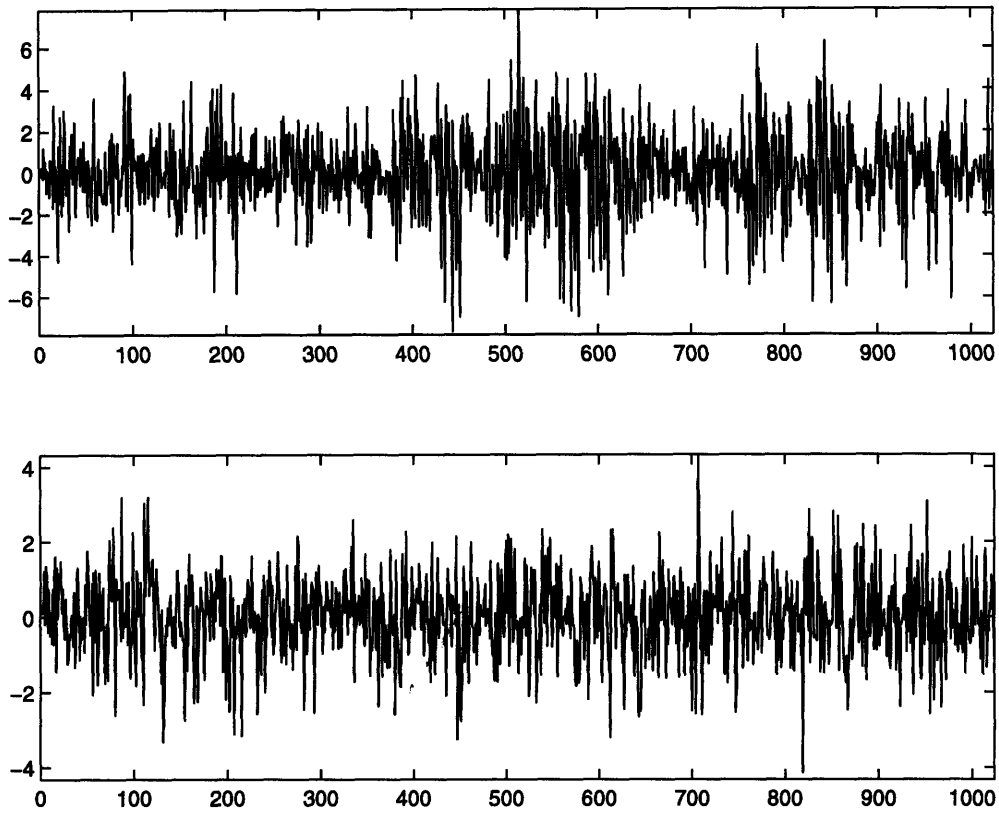


Figure 3-2: Sample Paths of 2-Parameter Multiscale AR(1) Model with (a) $\Theta_2 = (.9,1)$ and (b) $\Theta_2 = (.3,1)$.

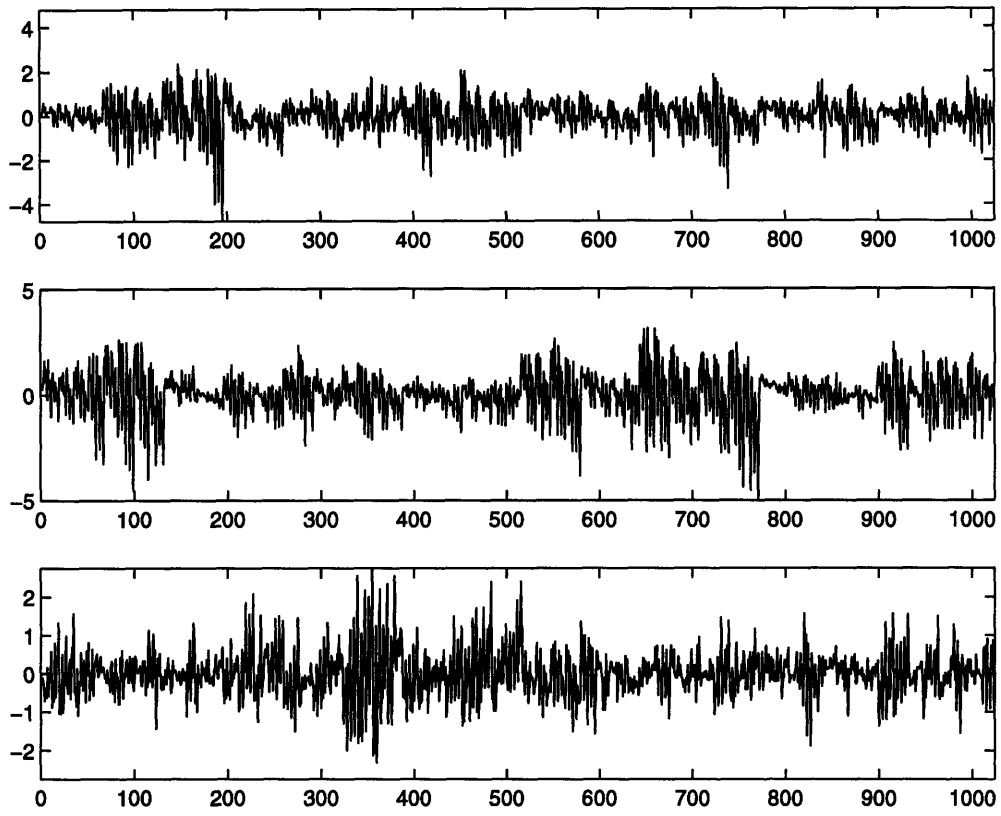


Figure 3-3: Sample Paths of 3-Parameter Multiscale AR(1) Model with (a) $\Theta_3 = (.9,1,.52)$, (b) $\Theta_3 = (.9,1,.5)$ and (c) $\Theta_3 = (.9,1,.48)$.

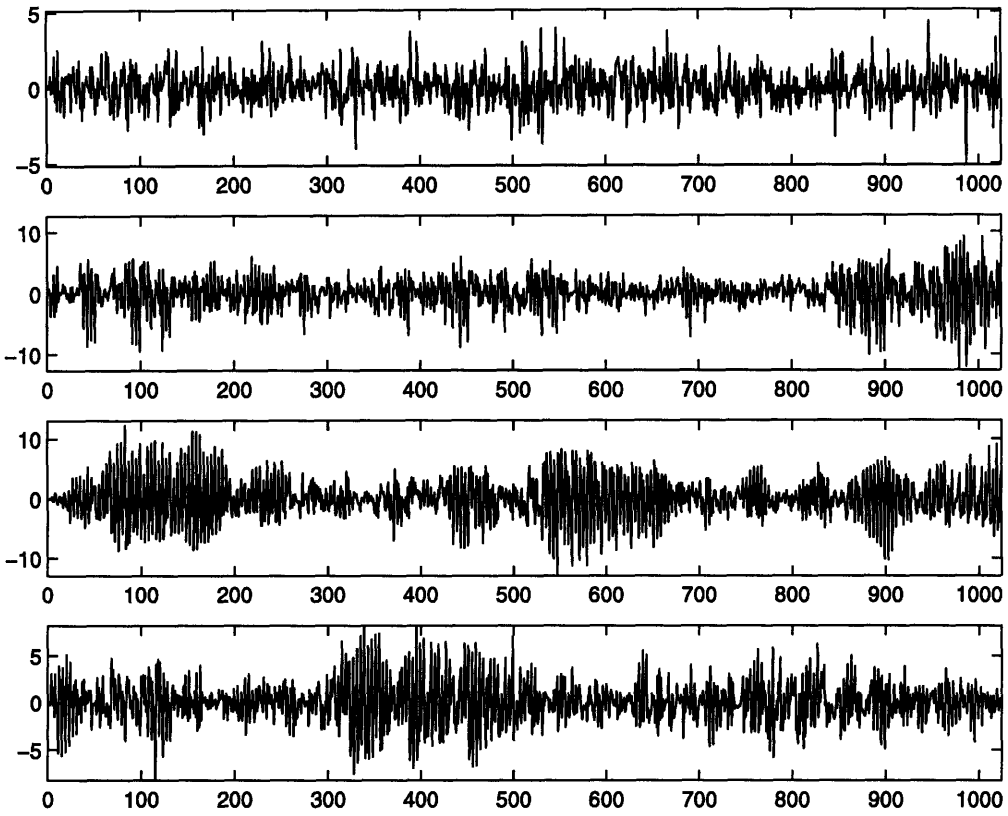


Figure 3-4: Sample Paths of 3-Parameter Multiscale AR(2) Model with (a) $\Theta_{3n} = (.5,.2,1)$, (b) $\Theta_{3n} = (.8,.2,1)$, (c) $\Theta_{3n} = (.2,.8,1)$ and (d) $\Theta_{3n} = (.5,.5,1)$.

## 3.4 Parameter Estimation

In Section 3.3, we described three multiresolution autoregressive stochastic models for use in this thesis. Below is the presentation of the parameter estimation techniques used to estimate the parameters of the three models. For each model, we take advantage of the fact that we are driving a filter with zero-mean, white Gaussian noise. Due to this fact, we can conclude that all of the wavelet coefficients are indeed zero-mean and that the are jointly Gaussian. Due to the fact that these coefficients are jointly Gaussian, we can use linear least square error (LLSE) estimation. Given that the wavelet coefficients are jointly Gaussian, we can conclude that the LLSE estimate is, in fact, optimal in the minimum mean square error (MMSE) sense.

LLSE estimation tells us that:

$$\hat{X}_{LLSE} = E[X|Y] = E[XY^T](E[YY^T])^{-1}\ Y, \tag{3.6}$$

where we denote $X$ as the wavelet coefficient being modeled and $Y$ represents either the scalar or vector information on which our model is based. In other words, $Y$ is scalar for AR(1) and is, in fact, just $x_{\hat{\gamma}t}$, while $Y$ is a vector representing both the parent node and the left neighbor on the same scale for the AR(2) model.

By extending Equation 3.6 to each of our models, we are able to estimate the $a$'s. Since $w_t$ is a zero-mean, white Gaussian noise process, we can conclude that:

$$A = E[XY^T](E[YY^T])^{-1}, \tag{3.7}$$

where A is either scalar or the row vector parameterization of the $a$'s. Having provided a means of estimating the $a$'s, we now turn our attention to estimating the standard deviation of the noise, i.e. $b$ and $b2^{-\frac{\lambda m}{2}}$. We begin this estimation by examining the second moment of each side of Equations 3.3 - 3.5.

For the 2-parameter AR(1) model, we have:

$$E[X^2] = a^2E[Y^2] + b^2 \tag{3.8}$$

from which we can immediately solve for $b$ as follows:

$$b = \sqrt{E[X^2] - a^2 E[Y^2]}. \tag{3.9}$$

For the 3-parameter AR(2) model, we have an equally simple estimation, given by:

$$E[X^2] = E[(AY)^2] + b^2 = a_1^2 E[Y_1^2] + a_2^2 E[Y_2^2] + a_1 a_2 E[Y_1 Y_2] + b^2. \tag{3.10}$$

Again solving for $b$, we get:

$$b = \sqrt{E[X^2] - a_1^2 E[Y_1^2] - a_2^2 E[Y_2^2] - a_1 a_2 E[Y_1 Y_2]}. \tag{3.11}$$

The 3-parameter AR(1) model is the only model that introduces complications in this estimation.

$$E[X^2] = a^2 E[Y^2] + b^2 2^{-\lambda m} \tag{3.12}$$

By taking $\log_2$ of either side of this equation, we are able to get a simple set of points that we can use regression to solve for $\lambda$ and $b$

$$\log_2\{E[X^2] - a^2 E[Y^2]\} = 2\log_2 b - \lambda m. \tag{3.13}$$

Lastly, we notice that $X$ and $Y$ are identically distributed for a given scale and therefore, we can represent Equation 3.13 as:

$$\log_2\{E[X_m^2] - a^2 E[X_{m-1}^2]\} = 2\log_2 b - \lambda m, \tag{3.14}$$

which serves as a final parameterization.

These parameter estimation algorithms will be used in Chapter 5 for the estimation of these models for various stocks, indices and foreign exchange data.

# Chapter 4

# Multiresolution Analysis of Financial Data

## 4.1 Common Stock Data

### 4.1.1 Description

The sample data used in this study consists of the daily returns on ten common stocks and three indices from June 14, 1963 to December 29, 1995. This period provides us with 8192 ($2^{13}$) sample points. The source of the data is the Center for Research in Security Prices (CRSP). Table 4.1 lists the stocks that were used, as well as their CUSIP numbers and ticker symbols.

Three indices are used in the analysis of stocks as well, the CRSP equal-weighted (CRSPEW), CRSP value-weighted (CRSPVW) and Standard & Poor's 500 (SP500).

All data is expressed in terms of the natural logarithm of the daily returns. This form is chosen due to the apparent lognormal density of stock returns. It is important to note that we are using a very large data set and that this fact calls the stationarity of the data into question. In response to this concern, we note that the wavelet transform, unlike many Fourier techniques, does not assume stationarity of the data.

| CUSIP # | STOCK NAME | TICKER SYMBOL |
|---|---|---|
| 01951210 | Allied Signal Inc | ALD |
| 42705610 | Hercules Inc | HPC |
| 45920010 | International Business Machines Corp | IBM |
| 19121610 | Coca Cola Co | KO |
| 71815410 | Phillip Morris Cos Inc | MO |
| 74740210 | Quaker Oats Co | OAT |
| 72481910 | Pittsburgh & West Virginia RR | PW |
| 88250810 | Texas Instruments Inc | TXN |
| 90254950 | U A L Corp | UAL |
| 30229010 | Exxon Corp | XON |

Table 4.1: Stock Listing

### 4.1.2 Wavelet Coefficient Statistics

As discussed in Section 2.2, the goal of multiresolution analysis is somewhat subjective. For the purpose of guiding the modeling of financial time series as multiscale stochastic processes, we direct our attention to the statistics of the wavelet coefficients and any detectable patterns within the coefficients. Tables 4.1-4.13 specify the mean, the standard deviation and the first five terms of the autocorrelation function for the stocks and indices as various scales. The Daubechies wavelet with three vanishing moments was used for the analysis. Figure 4.1.2 shows pictures of the corresponding scaling function and mother wavelet.

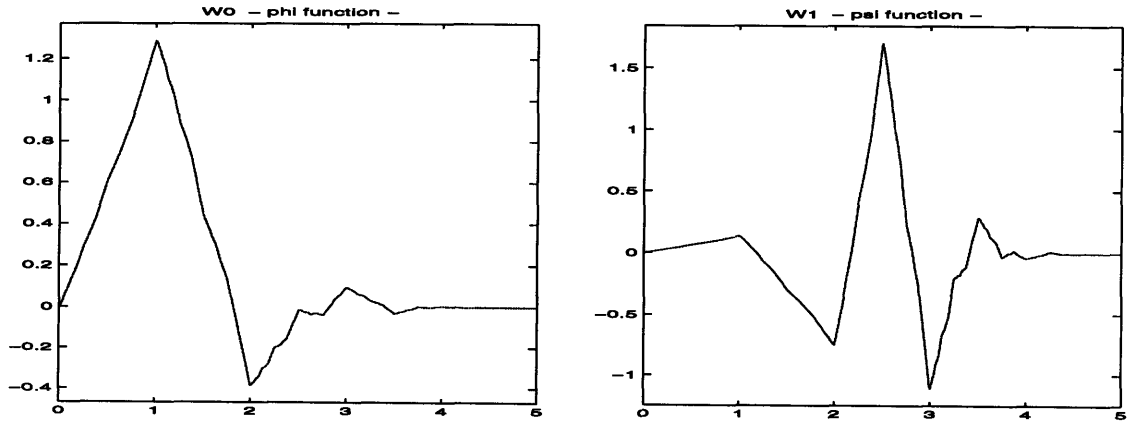


Figure 4-1: Scaling Function and Mother Wavelet for Daubechies 3

| | d6 | d5 | d4 | d3 | d2 | d1 |
|---|---|---|---|---|---|---|
| mean | -0.00197 | 0.00128 | 0.00058 | 0.00025 | -0.00010 | 0.00012 |
| std | 0.01252 | 0.01029 | 0.01005 | 0.00924 | 0.00873 | 0.00740 |
| r(0) | 1.00000 | 1.00000 | 1.00000 | 1.00000 | 1.00000 | 1.00000 |
| r(1) | -0.13788 | 0.16983 | 0.06875 | -0.02792 | -0.06153 | -0.14654 |
| r(2) | 0.11029 | 0.02665 | 0.01474 | -0.00259 | -0.01518 | 0.02493 |
| r(3) | -0.02093 | -0.10451 | 0.02026 | -0.01789 | 0.01232 | -0.03845 |
| r(4) | -0.03392 | -0.09876 | 0.05315 | 0.04974 | 0.02731 | -0.00304 |

Table 4.2: Wavelet Coefficient Statistics at Various Levels for CRSPEW

| | d6 | d5 | d4 | d3 | d2 | d1 |
|---|---|---|---|---|---|---|
| mean | -0.00156 | 0.00129 | 0.00057 | 0.00025 | -0.00006 | 0.00010 |
| std | 0.01029 | 0.00920 | 0.00979 | 0.00915 | 0.00909 | 0.00801 |
| r(0) | 1.00000 | 1.00000 | 1.00000 | 1.00000 | 1.00000 | 1.00000 |
| r(1) | -0.13233 | 0.22054 | 0.11984 | 0.02860 | -0.05157 | -0.10151 |
| r(2) | 0.05782 | 0.06403 | 0.03869 | -0.02306 | -0.00566 | -0.00731 |
| r(3) | -0.00860 | -0.05618 | 0.03398 | -0.00255 | 0.01454 | -0.03284 |
| r(4) | -0.08749 | -0.08156 | 0.02834 | 0.04322 | 0.04239 | -0.00760 |

Table 4.3: Wavelet Coefficient Statistics at Various Levels for CRSPVW

| | d6 | d5 | d4 | d3 | d2 | d1 |
|---|---|---|---|---|---|---|
| mean | -0.00167 | 0.00131 | 0.00055 | 0.00026 | -0.00005 | 0.00011 |
| std | 0.01034 | 0.00919 | 0.00973 | 0.00914 | 0.00913 | 0.00811 |
| r(0) | 1.00000 | 1.00000 | 1.00000 | 1.00000 | 1.00000 | 1.00000 |
| r(1) | -0.11964 | 0.22113 | 0.11786 | 0.03317 | -0.04959 | -0.09995 |
| r(2) | 0.06525 | 0.06838 | 0.04330 | -0.02559 | -0.00609 | -0.00792 |
| r(3) | 0.00011 | -0.05557 | 0.03102 | -0.00254 | 0.01422 | -0.03463 |
| r(4) | -0.07847 | -0.08234 | 0.02041 | 0.04384 | 0.04312 | -0.00853 |

Table 4.4: Wavelet Coefficient Statistics at Various Levels for SP500

| | d6 | d5 | d4 | d3 | d2 | d1 |
|---|---|---|---|---|---|---|
| mean | -0.00075 | 0.00285 | 0.00091 | -0.00021 | -0.00030 | 0.00018 |
| std | 0.01715 | 0.01501 | 0.01674 | 0.01818 | 0.01892 | 0.01725 |
| r(0) | 1.00000 | 1.00000 | 1.00000 | 1.00000 | 1.00000 | 1.00000 |
| r(1) | -0.04745 | -0.09624 | 0.03695 | -0.01576 | -0.04355 | -0.01478 |
| r(2) | 0.07671 | 0.11820 | 0.00970 | -0.01248 | -0.00324 | -0.01299 |
| r(3) | -0.03820 | -0.13292 | -0.08951 | -0.06155 | 0.06137 | -0.02858 |
| r(4) | -0.23057 | -0.10208 | 0.05756 | 0.02705 | -0.06087 | -0.01096 |

Table 4.5: Wavelet Coefficient Statistics at Various Levels for ALD

| | d6 | d5 | d4 | d3 | d2 | d1 |
|---|---|---|---|---|---|---|
| mean | -0.00166 | 0.00210 | 0.00067 | -0.00039 | 0.00013 | -0.00007 |
| std | 0.01814 | 0.01628 | 0.01812 | 0.01841 | 0.01680 | 0.01580 |
| r(0) | 1.00000 | 1.00000 | 1.00000 | 1.00000 | 1.00000 | 1.00000 |
| r(1) | 0.00906 | 0.09574 | 0.00922 | 0.01705 | -0.04753 | -0.09085 |
| r(2) | -0.03450 | 0.03381 | 0.01680 | 0.00475 | -0.03271 | -0.01139 |
| r(3) | 0.06558 | -0.01469 | 0.00405 | 0.01310 | 0.01975 | 0.00202 |
| r(4) | -0.16809 | 0.15455 | -0.02142 | 0.03240 | 0.00552 | -0.00711 |

Table 4.6: Wavelet Coefficient Statistics at Various Levels for HPC

| | d6 | d5 | d4 | d3 | d2 | d1 |
|---|---|---|---|---|---|---|
| mean | 0.00043 | 0.00198 | 0.00087 | 0.00027 | -0.00010 | 0.00007 |
| std | 0.01449 | 0.01399 | 0.01346 | 0.01388 | 0.01465 | 0.01424 |
| r(0) | 1.00000 | 1.00000 | 1.00000 | 1.00000 | 1.00000 | 1.00000 |
| r(1) | 0.05460 | 0.00990 | 0.11251 | -0.00290 | -0.01520 | -0.02376 |
| r(2) | -0.07275 | 0.12025 | -0.01832 | -0.02228 | -0.00722 | -0.02403 |
| r(3) | 0.07398 | -0.01784 | 0.06538 | -0.01842 | -0.00488 | -0.03264 |
| r(4) | 0.01368 | -0.06837 | -0.02346 | 0.00528 | 0.02154 | 0.00288 |

Table 4.7: Wavelet Coefficient Statistics at Various Levels for IBM

| | d6 | d5 | d4 | d3 | d2 | d1 |
|---|---|---|---|---|---|---|
| mean | -0.00055 | 0.00031 | 0.00055 | 0.00022 | -0.00063 | 0.00017 |
| std | 0.01405 | 0.01330 | 0.01571 | 0.01555 | 0.01581 | 0.01458 |
| r(0) | 1.00000 | 1.00000 | 1.00000 | 1.00000 | 1.00000 | 1.00000 |
| r(1) | -0.04991 | 0.03718 | 0.15873 | 0.00622 | -0.01023 | -0.05210 |
| r(2) | -0.01129 | 0.01708 | -0.03291 | 0.00698 | -0.02405 | -0.02530 |
| r(3) | -0.09513 | 0.12257 | 0.01962 | 0.03389 | -0.01905 | -0.02213 |
| r(4) | 0.12624 | -0.03633 | -0.02112 | 0.03738 | 0.04143 | -0.02008 |

Table 4.8: Wavelet Coefficient Statistics at Various Levels for KO

| | d6 | d5 | d4 | d3 | d2 | d1 |
|---|---|---|---|---|---|---|
| mean | -0.00204 | 0.00047 | -0.00038 | 0.00045 | -0.00006 | 0.00004 |
| std | 0.01502 | 0.01432 | 0.01716 | 0.01720 | 0.01636 | 0.01481 |
| r(0) | 1.00000 | 1.00000 | 1.00000 | 1.00000 | 1.00000 | 1.00000 |
| r(1) | -0.11450 | 0.09086 | 0.09431 | -0.08057 | -0.03416 | -0.03626 |
| r(2) | 0.19079 | -0.01166 | 0.04858 | -0.01643 | -0.01559 | 0.00752 |
| r(3) | -0.21148 | 0.00954 | -0.04601 | 0.04063 | -0.00931 | -0.00243 |
| r(4) | 0.01706 | -0.04112 | -0.06917 | 0.04263 | 0.00599 | 0.02831 |

Table 4.9: Wavelet Coefficient Statistics at Various Levels for MO

| | d6 | d5 | d4 | d3 | d2 | d1 |
|---|---|---|---|---|---|---|
| mean | -0.00110 | 0.00244 | 0.00046 | 0.00007 | -0.00030 | 0.00056 |
| std | 0.01753 | 0.01645 | 0.01756 | 0.01715 | 0.01801 | 0.01679 |
| r(0) | 1.00000 | 1.00000 | 1.00000 | 1.00000 | 1.00000 | 1.00000 |
| r(1) | -0.05885 | 0.07211 | 0.05062 | 0.01634 | 0.00923 | -0.04505 |
| r(2) | -0.05092 | -0.06392 | 0.06224 | -0.00524 | 0.00984 | -0.00969 |
| r(3) | -0.07547 | -0.06734 | -0.06914 | 0.01325 | -0.00018 | 0.02005 |
| r(4) | 0.15724 | -0.00410 | 0.03038 | 0.03230 | 0.00107 | -0.00770 |

Table 4.10: Wavelet Coefficient Statistics at Various Levels for OAT

| | d6 | d5 | d4 | d3 | d2 | d1 |
|---|---|---|---|---|---|---|
| mean | 0.00023 | 0.00040 | -0.00060 | 0.00042 | -0.00064 | -0.00025 |
| std | 0.01225 | 0.01227 | 0.01193 | 0.01517 | 0.01718 | 0.02181 |
| r(0) | 1.00000 | 1.00000 | 1.00000 | 1.00000 | 1.00000 | 1.00000 |
| r(1) | -0.18093 | 0.07747 | 0.00391 | 0.10538 | 0.09323 | 0.09464 |
| r(2) | -0.07695 | -0.02953 | 0.05447 | -0.07807 | -0.02548 | -0.01474 |
| r(3) | 0.16129 | -0.00753 | 0.02376 | 0.02522 | 0.02156 | -0.00023 |
| r(4) | -0.07171 | 0.01946 | 0.00842 | 0.02374 | -0.00431 | 0.00704 |

Table 4.11: Wavelet Coefficient Statistics at Various Levels for PW

| | d6 | d5 | d4 | d3 | d2 | d1 |
|---|---|---|---|---|---|---|
| mean | -0.00285 | 0.00225 | 0.00024 | 0.00077 | -0.00016 | 0.00039 |
| std | 0.02183 | 0.02206 | 0.02190 | 0.02310 | 0.02224 | 0.02035 |
| r(0) | 1.00000 | 1.00000 | 1.00000 | 1.00000 | 1.00000 | 1.00000 |
| r(1) | 0.11402 | 0.04423 | 0.01862 | -0.06777 | -0.01953 | -0.04851 |
| r(2) | 0.06264 | 0.00597 | 0.03724 | 0.02803 | 0.00215 | 0.03338 |
| r(3) | 0.03618 | -0.08250 | 0.05535 | -0.06086 | -0.01969 | -0.02344 |
| r(4) | -0.03258 | 0.11451 | -0.06682 | 0.01076 | 0.00867 | 0.00124 |

Table 4.12: Wavelet Coefficient Statistics at Various Levels for TXN

| | d6 | d5 | d4 | d3 | d2 | d1 |
|---|---|---|---|---|---|---|
| mean | -0.00257 | 0.00176 | 0.00037 | 0.00140 | -0.00028 | 0.00040 |
| std | 0.02788 | 0.02357 | 0.02598 | 0.02723 | 0.02487 | 0.02499 |
| r(0) | 1.00000 | 1.00000 | 1.00000 | 1.00000 | 1.00000 | 1.00000 |
| r(1) | -0.01423 | 0.13872 | 0.04852 | -0.03045 | -0.07207 | 0.01256 |
| r(2) | -0.06882 | -0.03418 | -0.02009 | 0.00556 | 0.00980 | 0.03073 |
| r(3) | 0.06225 | -0.09090 | -0.02547 | -0.00422 | -0.00736 | -0.02146 |
| r(4) | -0.12363 | 0.01415 | 0.04049 | -0.05821 | 0.02191 | 0.01419 |

Table 4.13: Wavelet Coefficient Statistics at Various Levels for UAL

| | d6 | d5 | d4 | d3 | d2 | d1 |
|---|---|---|---|---|---|---|
| mean | -0.00302 | 0.00161 | 0.00040 | 0.00028 | 0.00008 | -0.00002 |
| std | 0.01054 | 0.01085 | 0.01186 | 0.01306 | 0.01316 | 0.01230 |
| r(0) | 1.00000 | 1.00000 | 1.00000 | 1.00000 | 1.00000 | 1.00000 |
| r(1) | 0.03385 | 0.06535 | 0.11068 | 0.07202 | -0.05690 | -0.06150 |
| r(2) | -0.01512 | 0.13382 | -0.02529 | 0.00228 | 0.01105 | 0.00427 |
| r(3) | -0.11397 | 0.02599 | -0.01543 | 0.02542 | -0.03100 | -0.03538 |
| r(4) | -0.04082 | 0.03092 | 0.03011 | 0.01716 | 0.09080 | 0.00165 |

Table 4.14: Wavelet Coefficient Statistics at Various Levels for XON

The autocorrelation function of the wavelet coefficients in Tables 4.2-4.14 should be of particular interest due to our intension to model these coefficients as the output of an all-pole filter. The correlation at lag one, r(1), appears across scales for our three indices, yet rarely in our stocks. In all other cases, we see a more uncorrelated representation. In terms of our multiscale autoregressive models, wavelet coefficients on the same scale only affect models of order greater than one. This leads us to believe that an AR(1) model for the wavelet coefficients of stocks would appear appropriate. Similarly, we would expect to need an AR(2) model to represent the behavior of the indices.

Another means of analyzing the statistics of wavelet coefficients is through the use of the scalogram (Section 2.2.2). The scalograms presented in Figures 4-2 - 4-14 visually display the energy in the wavelet coefficients at each scale. These scalograms offer insight into how we can model the multiscale process to be driven by noise with scale-dependent variance. We can see from the scalograms Figures 4-2 - 4-14 that most stocks display a slight positive slope, which means more variation at finer scales.

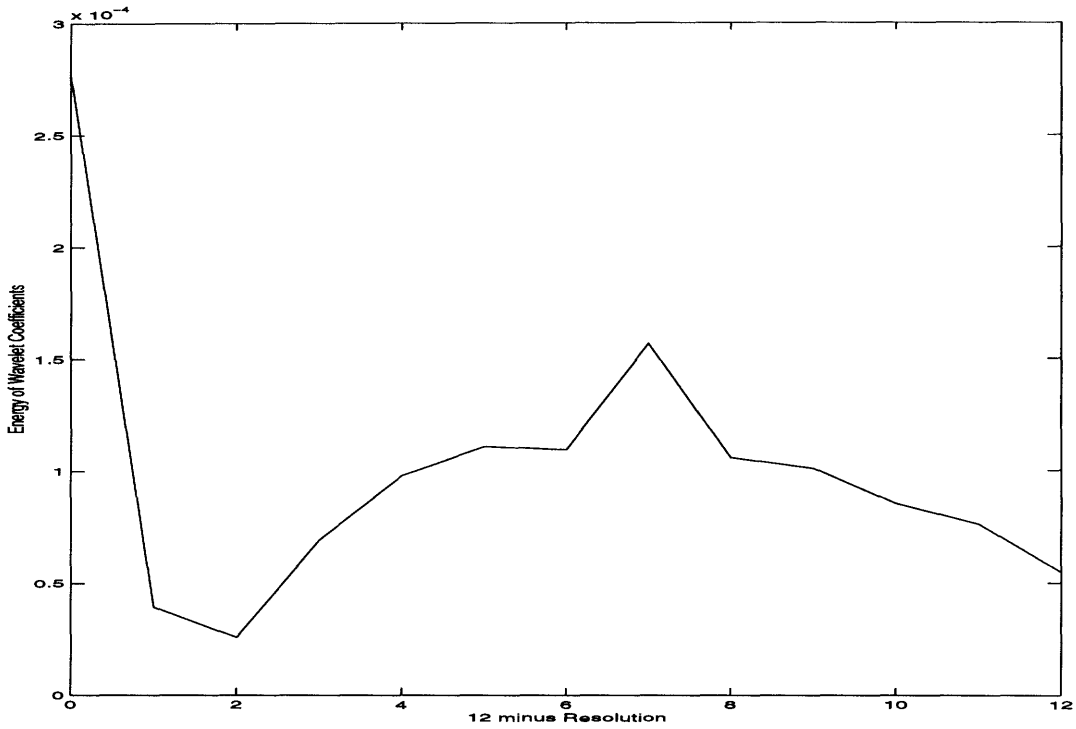


Figure 4-2: Wavelet Scalogram for CRSPEW

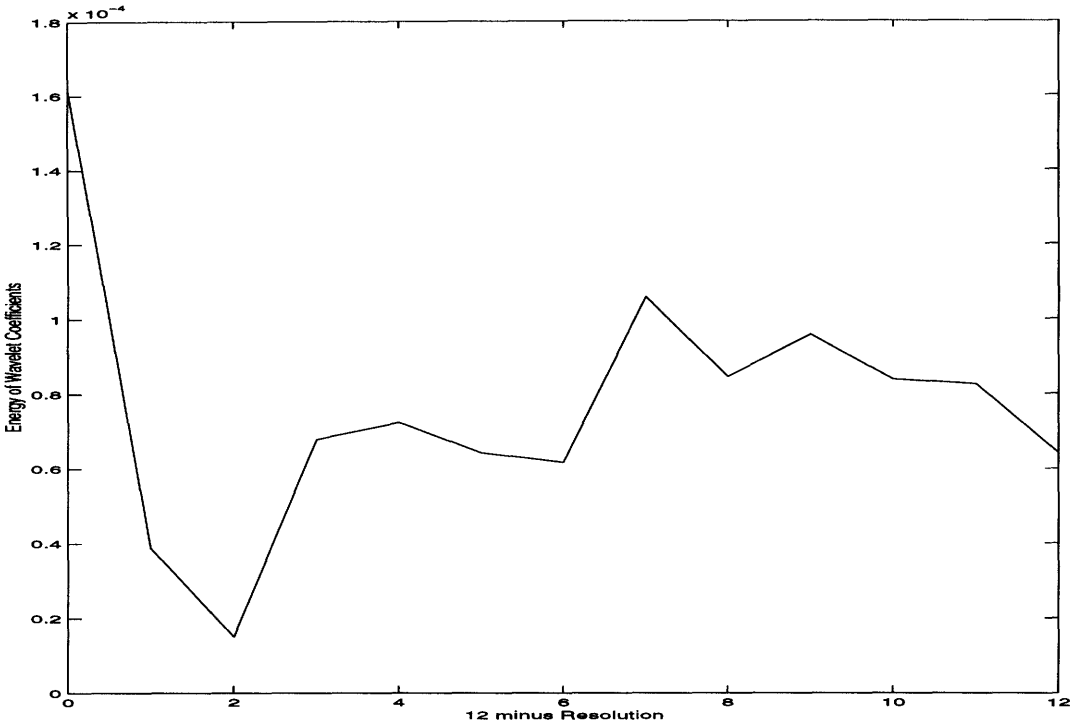


Figure 4-3: Wavelet Scalogram for CRSPVW

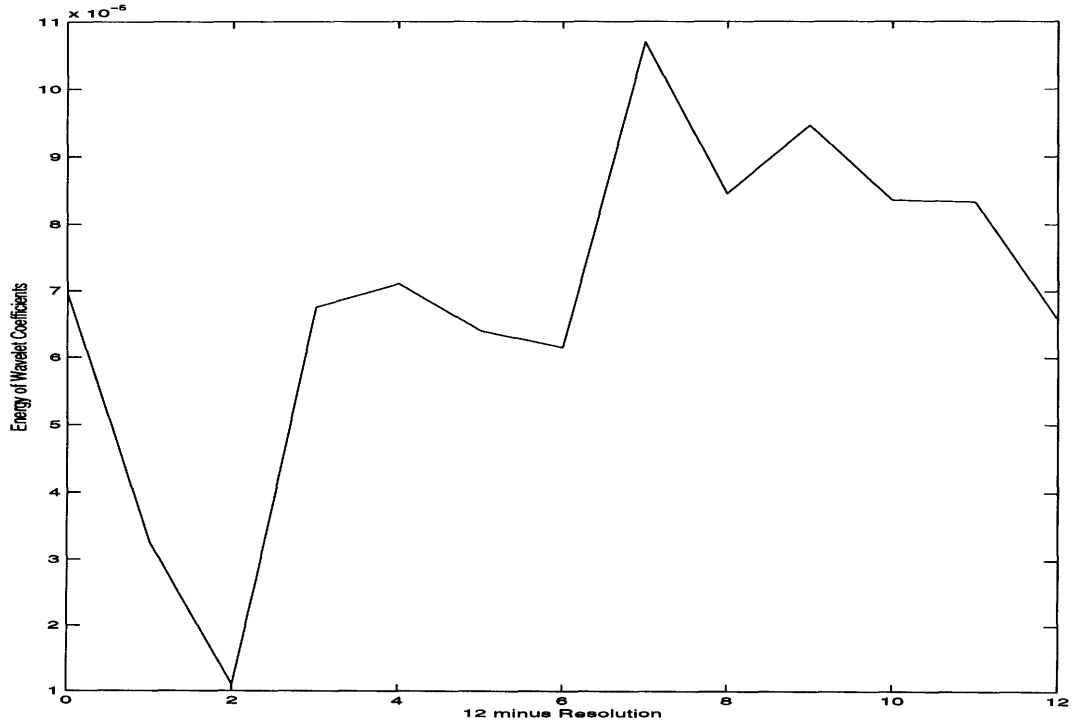


Figure 4-4: Wavelet Scalogram for SP500

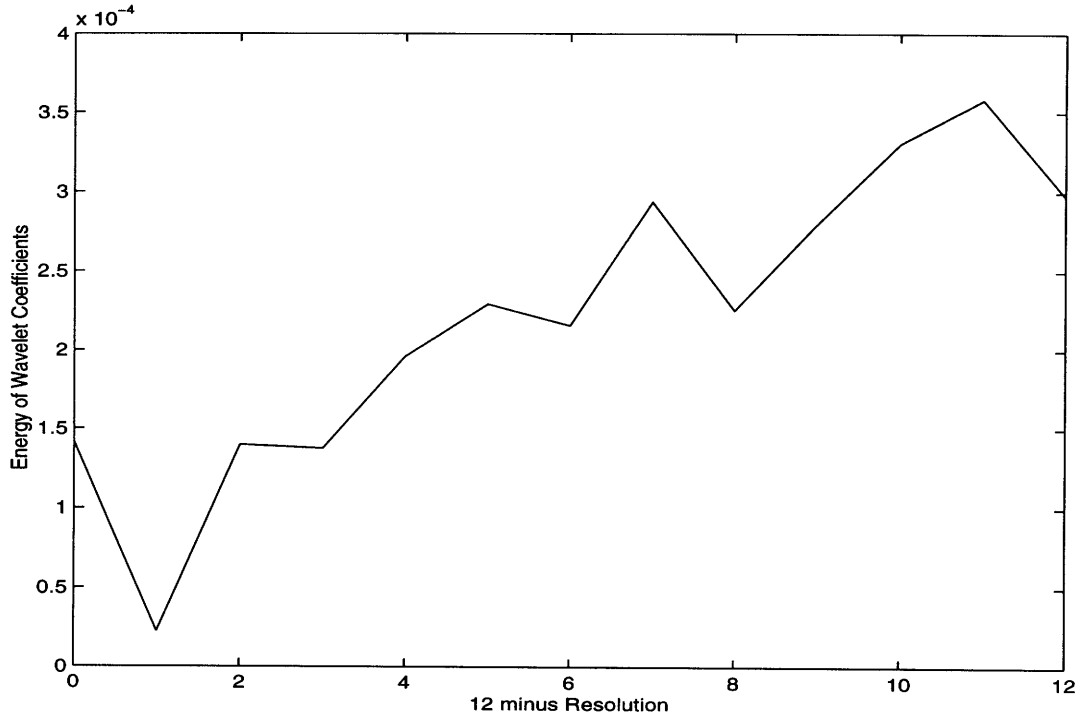


Figure 4-5: Wavelet Scalogram for ALD

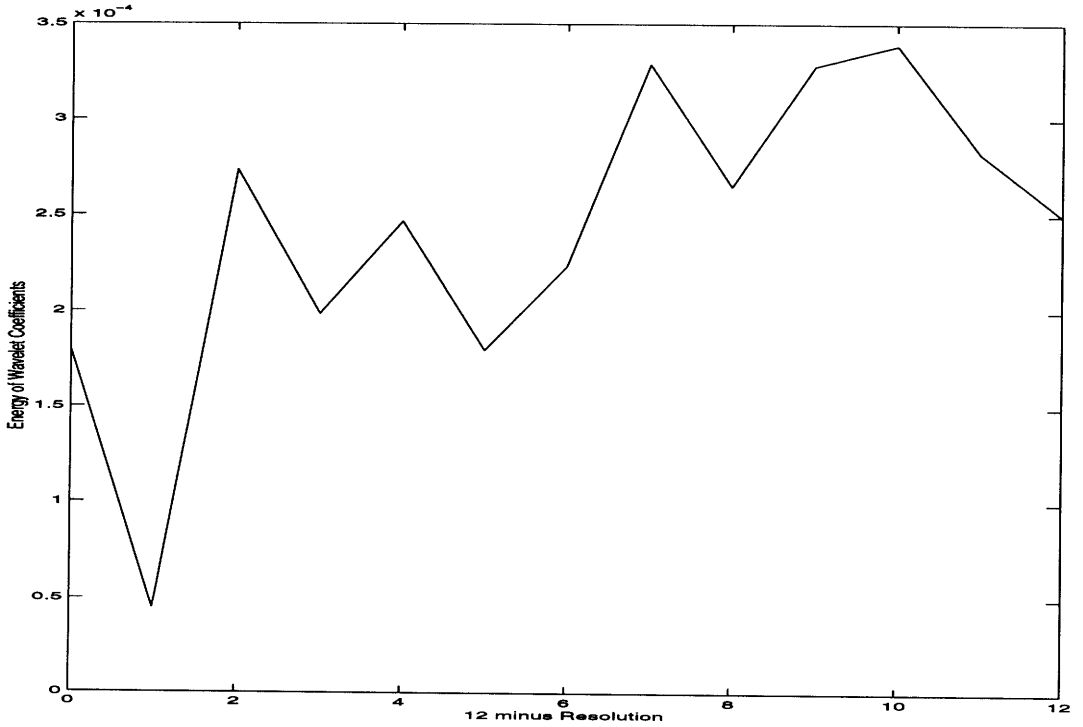


Figure 4-6: Wavelet Scalogram for HPC

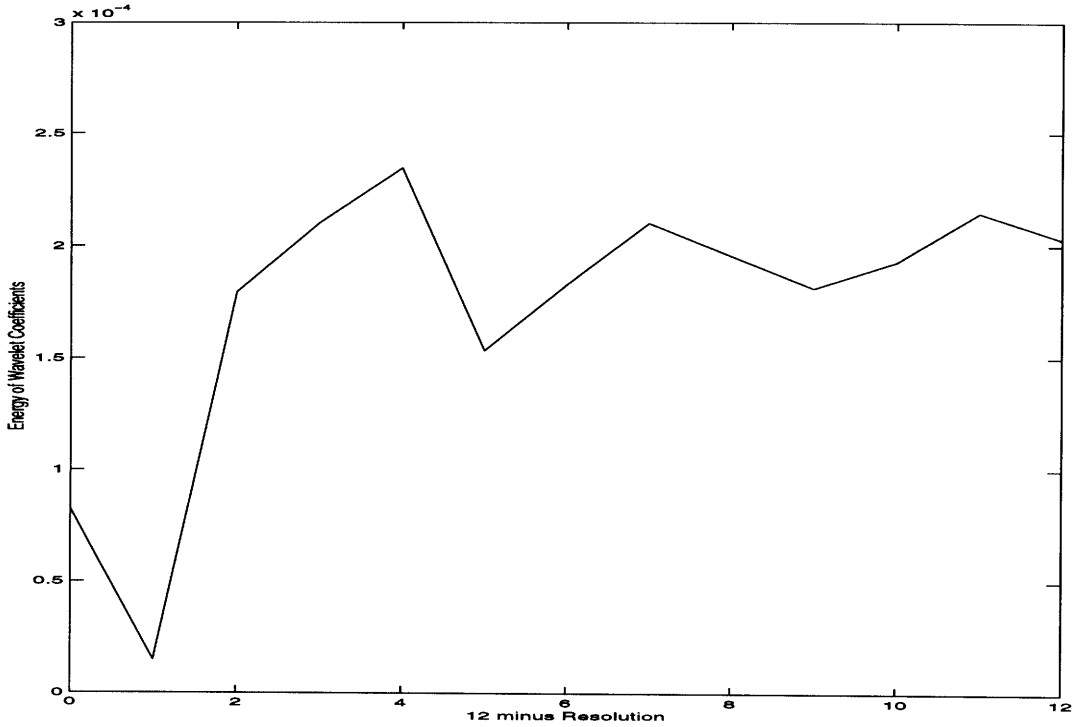


Figure 4-7: Wavelet Scalogram for IBM

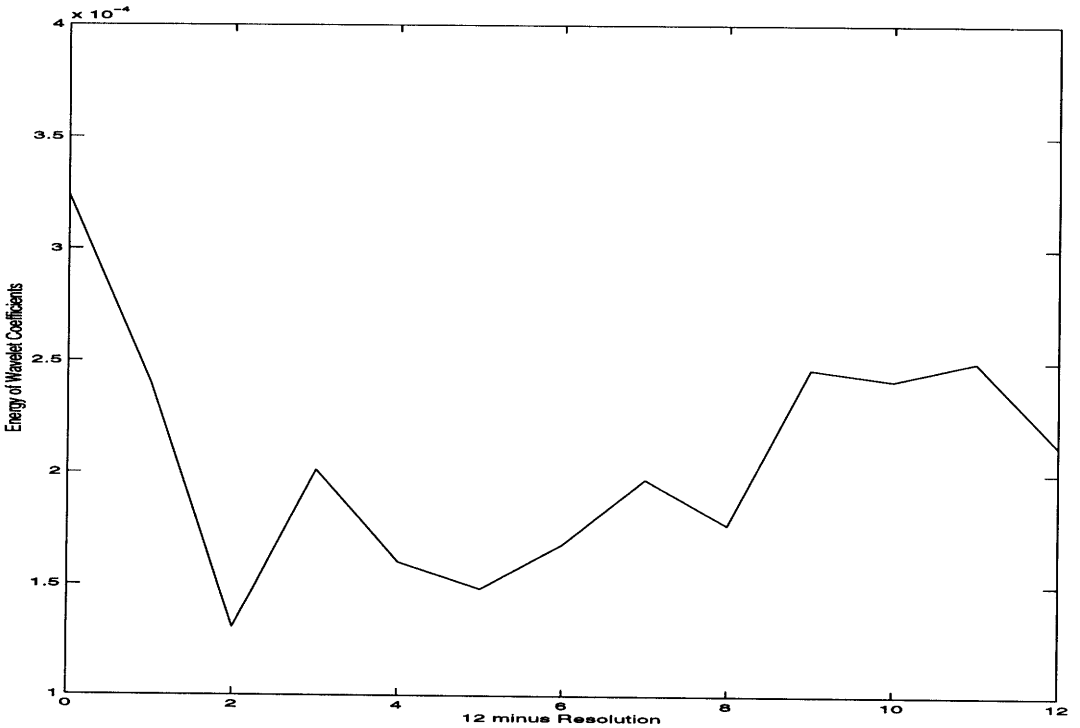


Figure 4-8: Wavelet Scalogram for KO

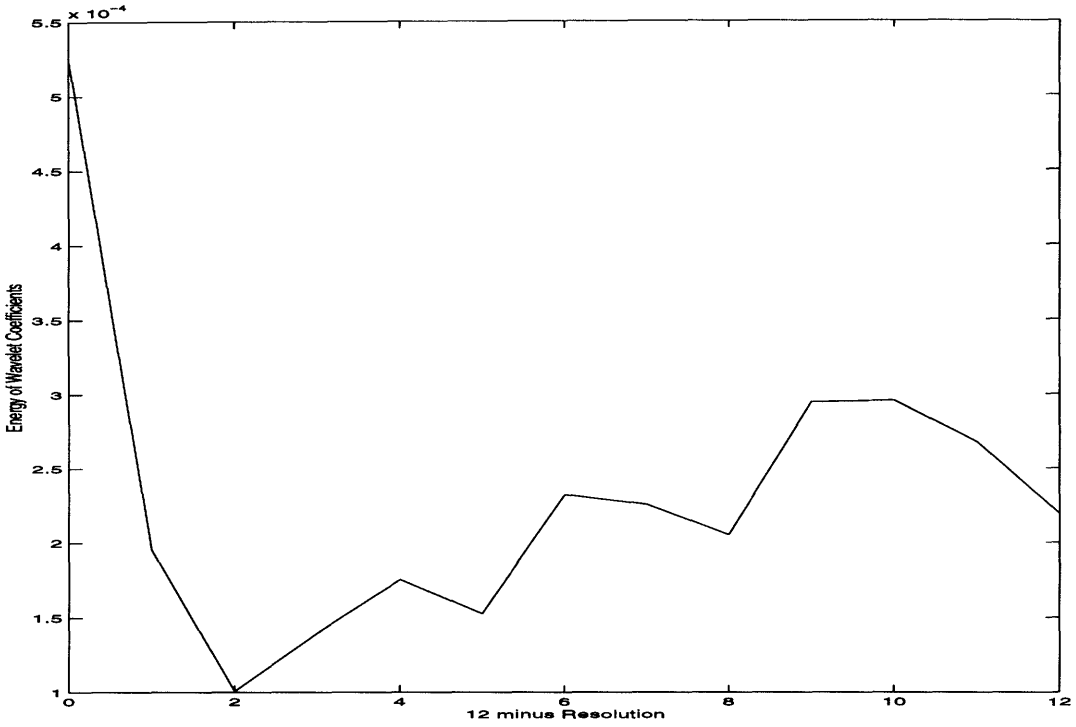


Figure 4-9: Wavelet Scalogram for MO

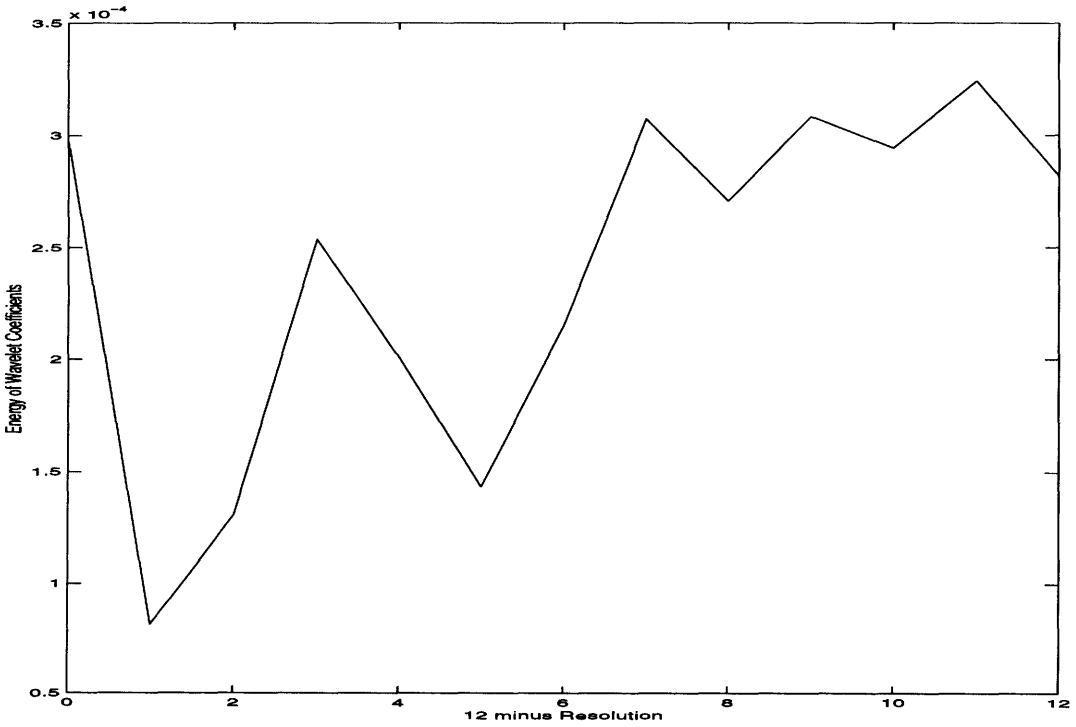


Figure 4-10: Wavelet Scalogram for OAT

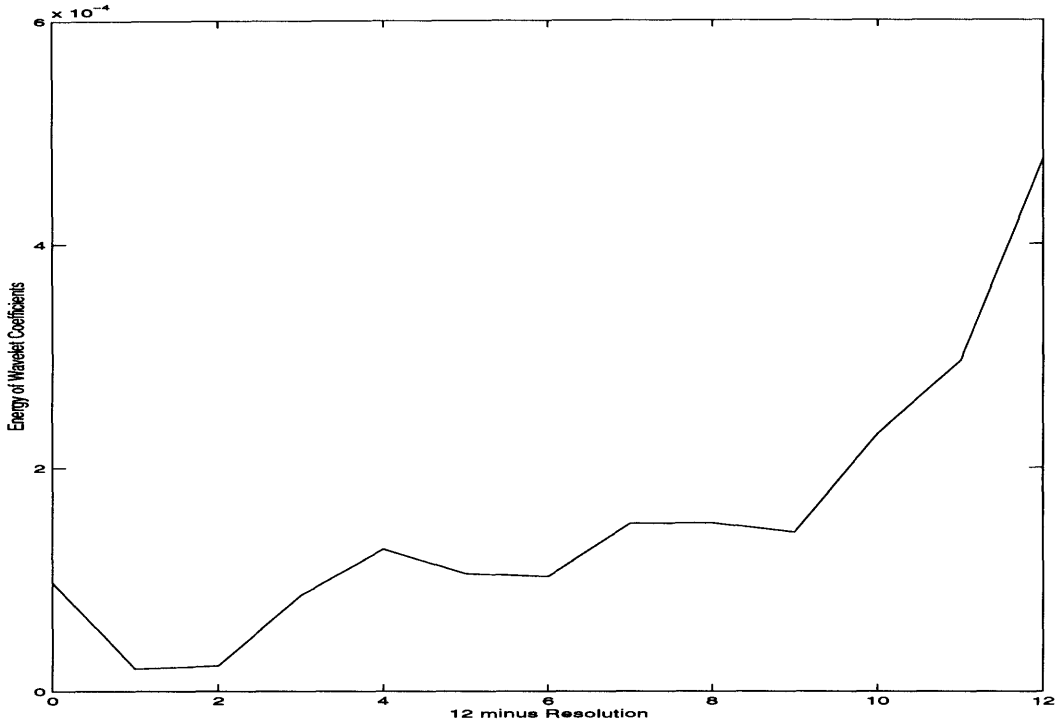


Figure 4-11: Wavelet Scalogram for PW

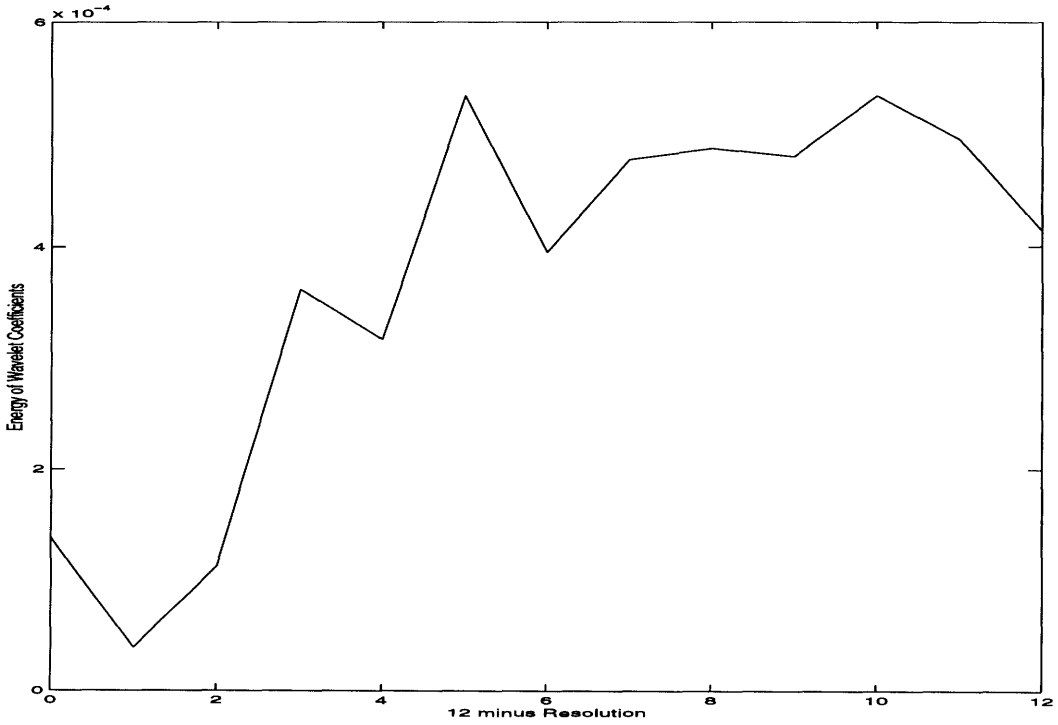


Figure 4-12: Wavelet Scalogram for TXN

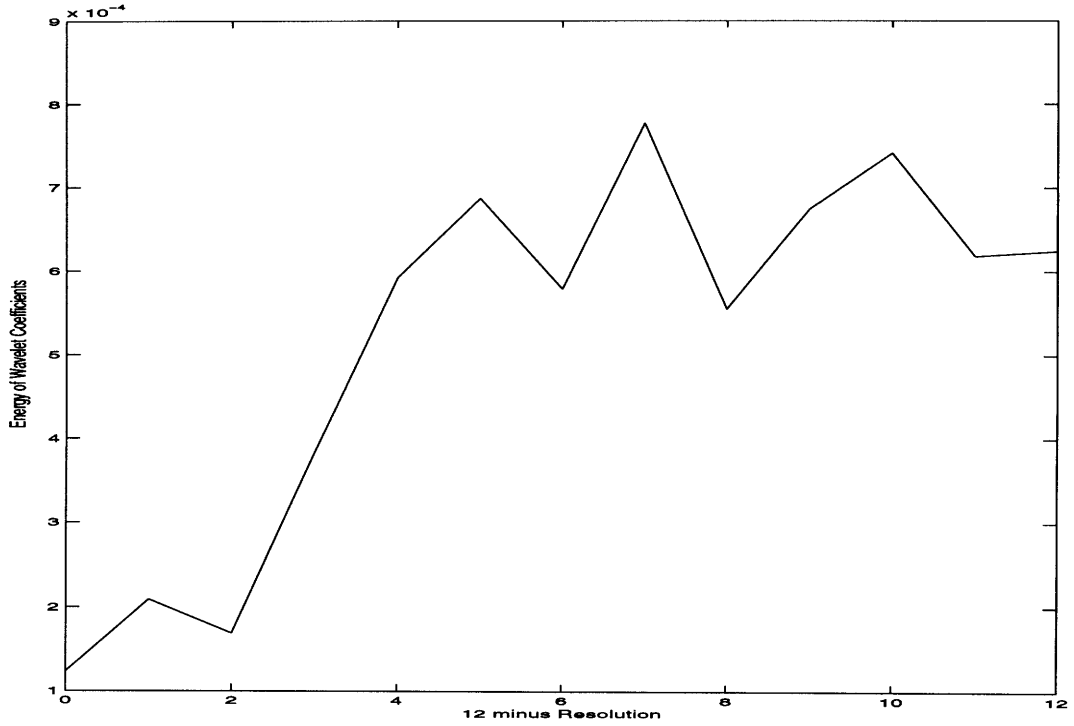


Figure 4-13: Wavelet Scalogram for UAL

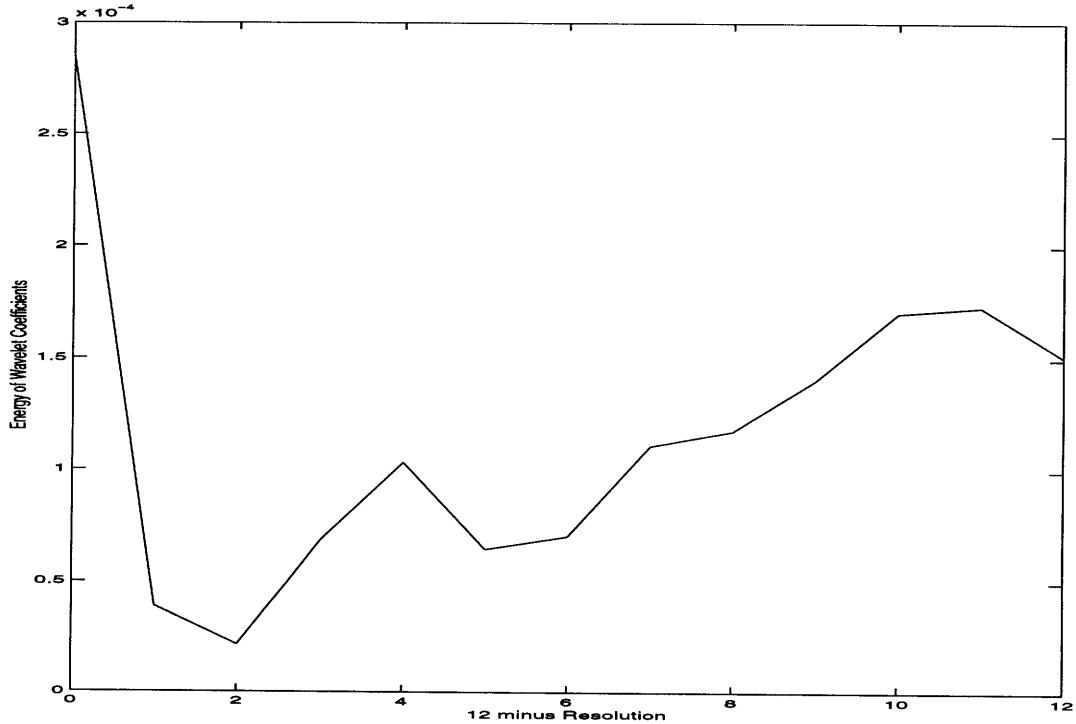


Figure 4-14: Wavelet Scalogram for XON

Yet another presentation of the wavelet coefficients is in the form of freqeuncy histograms. These histograms, which are displayed in Appendix A in Figures A-1 - A-13, offer insight into the density function of the wavelet coefficients. It can be seen that the Gaussian distribution is a good approximation for the wavelet coefficient densities. One must notice how the wavelet coefficients in finer scales are more well-behaved that those at coarser scales. This is both of function of the number of coefficients and their susceptability to edge effects.

The final means of viewing data is an extremely visual one. We plot all of the wavelets coefficients in the same picture. This picture is segmented according to dilation and translation. Each rectangular segment represents one coefficient. Clearly the finer scales have more coefficients than the coarser scales. Each rectangular segment is color-coded based on the absolute value of the wavelet coefficient at that position. This method allows one to visualize the evolution of wavelet coefficients across scale, especially when large shocks take place. Figure 4-14 and Figures B-1 - B-12 display these pictures for our stocks and indices.

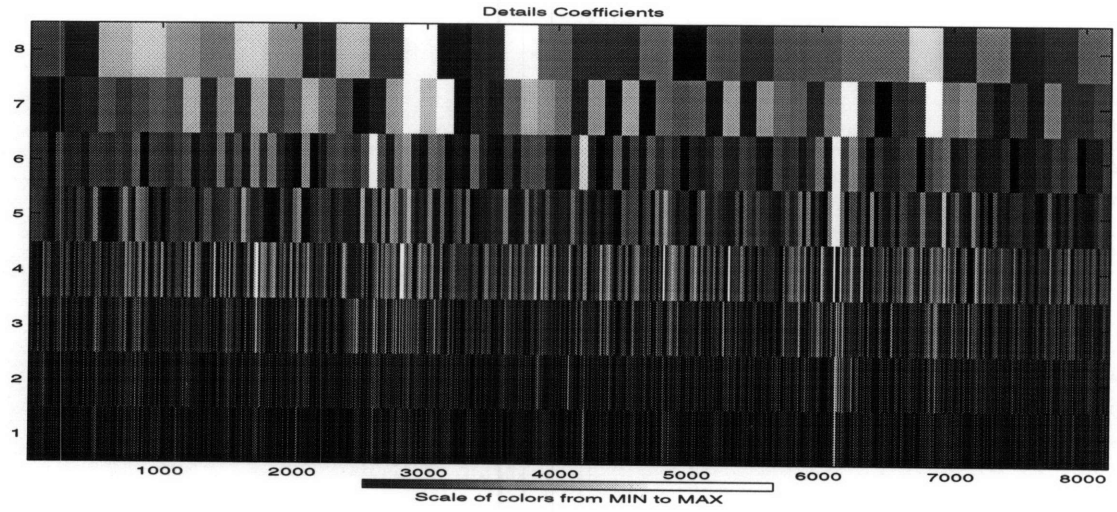


Figure 4-15: Wavelet Coefficient Intensity by Dilation and Translation for CRSPEW

## 4.2 Foreign Exchange Data

### 4.2.1 Description

The data used in this study consists of the tick-by-tick foreign exchange rate of the Japanese Yen to the US Dollar. The actual data gives the bid-ask spreads, however, we concentrate on the midpoint between these two values. The data is also unevenly sampled, in that the time interval between data points is constantly changing due to its tick-by-tick nature. Despite the slight abuse, we treat the data as if it were evenly sampled. The data comes from the Olsen & Associates Research Institute for Applied Economics HFDF data set. The data spans from October 1, 1992 to January 5, 1993. The result is 117966 data points. For the purpose of diversity we break the data up into six sets of 16384 ($2^{14}$) points. For the purpose of brevity, these will be labeled JPY/USD#1 through JPY/USD#6. The higher the number, the older the data. The log return of this series was used for the purpose of analysis.

### 4.2.2 Wavelet Coefficient Statistics

As with the individual stocks, the modeling of foreign exchange rates requires knowledge of the wavelet coefficient statistics by scale. Tables 4.15-4.20 show the mean, standard deviation, and the first five terms of the autocorrelation function. Since our six foreign exchange data sets came from the Yen/Dollar exchange, we would expect the statistics of the six sets to be similar. We observe some correlation between wavelet coefficients on the same scale. This event raises the expectation that an AR(2) multiscale model will be needed. One can also see from these tables the progression of standard deviations along scale. Clearly the finer the scale the greater the variance in the wavelet coefficients. This result can also be seen in the wavelet scalogram of the data in Figure 4-15. Figure 4-15 is the the scalogram of JPY/USD#1 and is indicative of the others.

| | d8 | d7 | d6 | d5 | d4 | d3 | d2 | d1 |
|---|---|---|---|---|---|---|---|---|
| mean | 0.00001 | -0.00000 | -0.00001 | 0.00001 | 0.00000 | 0.00000 | -0.00001 | 0.00000 |
| std | 0.00011 | 0.00011 | 0.00013 | 0.00014 | 0.00016 | 0.00023 | 0.00034 | 0.00050 |
| r(0) | 1.00000 | 1.00000 | 1.00000 | 1.00000 | 1.00000 | 1.00000 | 1.00000 | 1.00000 |
| r(1) | 0.06968 | 0.06200 | 0.08296 | -0.00710 | 0.00692 | 0.24879 | 0.22713 | 0.18966 |
| r(2) | 0.01980 | -0.13888 | 0.04152 | 0.02989 | -0.04427 | 0.06373 | -0.01760 | -0.01617 |
| r(3) | 0.08354 | -0.06653 | 0.09493 | -0.02580 | 0.04748 | 0.04941 | 0.00366 | -0.00816 |
| r(4) | 0.06714 | -0.00752 | -0.07660 | 0.06363 | -0.00298 | 0.04089 | 0.01788 | 0.00350 |

Table 4.15: Wavelet Coefficient Statistics at Various Levels for JPY/USD#1

| | d8 | d7 | d6 | d5 | d4 | d3 | d2 | d1 |
|---|---|---|---|---|---|---|---|---|
| mean | 0.00001 | 0.00001 | -0.00001 | -0.00001 | 0.00000 | -0.00000 | -0.00000 | -0.00001 |
| std | 0.00010 | 0.00011 | 0.00011 | 0.00012 | 0.00014 | 0.00020 | 0.00030 | 0.00047 |
| r(0) | 1.00000 | 1.00000 | 1.00000 | 1.00000 | 1.00000 | 1.00000 | 1.00000 | 1.00000 |
| r(1) | 0.24490 | 0.21315 | -0.01033 | 0.02332 | 0.05249 | 0.23747 | 0.19862 | 0.14620 |
| r(2) | 0.04727 | 0.09970 | 0.02030 | -0.09381 | -0.02333 | -0.00824 | -0.03383 | -0.03061 |
| r(3) | 0.00111 | -0.03473 | -0.09861 | 0.03223 | -0.03412 | -0.00495 | 0.01435 | 0.00227 |
| r(4) | 0.09031 | -0.11745 | -0.00366 | -0.07645 | 0.01345 | 0.00768 | -0.00483 | -0.00834 |

Table 4.16: Wavelet Coefficient Statistics at Various Levels for JPY/USD#2

| | d8 | d7 | d6 | d5 | d4 | d3 | d2 | d1 |
|---|---|---|---|---|---|---|---|---|
| mean | 0.00000 | -0.00000 | -0.00001 | -0.00000 | -0.00000 | -0.00000 | 0.00001 | 0.00001 |
| std | 0.00008 | 0.00009 | 0.00012 | 0.00011 | 0.00013 | 0.00020 | 0.00033 | 0.00044 |
| r(0) | 1.00000 | 1.00000 | 1.00000 | 1.00000 | 1.00000 | 1.00000 | 1.00000 | 1.00000 |
| r(1) | -0.17423 | -0.01930 | -0.03411 | 0.02076 | 0.13188 | 0.19803 | 0.20555 | 0.16587 |
| r(2) | 0.14629 | -0.25695 | -0.00615 | -0.05554 | -0.01874 | -0.00027 | -0.02683 | -0.02242 |
| r(3) | 0.04776 | 0.01192 | -0.05391 | -0.03767 | -0.05709 | 0.02258 | -0.01201 | -0.00560 |
| r(4) | 0.10200 | 0.10414 | -0.11471 | -0.06134 | -0.02487 | -0.03000 | -0.04497 | 0.01662 |

Table 4.17: Wavelet Coefficient Statistics at Various Levels for JPY/USD#3

| | d8 | d7 | d6 | d5 | d4 | d3 | d2 | d1 |
|---|---|---|---|---|---|---|---|---|
| mean | 0.00004 | -0.00000 | 0.00000 | -0.00000 | -0.00001 | 0.00001 | -0.00000 | -0.00000 |
| std | 0.00012 | 0.00013 | 0.00016 | 0.00013 | 0.00015 | 0.00020 | 0.00031 | 0.00047 |
| r(0) | 1.00000 | 1.00000 | 1.00000 | 1.00000 | 1.00000 | 1.00000 | 1.00000 | 1.00000 |
| r(1) | 0.09612 | 0.00643 | 0.02174 | 0.01051 | 0.14375 | 0.14494 | 0.17452 | 0.15064 |
| r(2) | -0.07404 | -0.01663 | 0.03295 | -0.06569 | -0.03427 | -0.04498 | -0.02292 | -0.04150 |
| r(3) | -0.06194 | 0.00356 | -0.00254 | 0.04013 | 0.02495 | 0.01552 | -0.00691 | 0.00773 |
| r(4) | -0.17000 | -0.02682 | -0.11541 | -0.02491 | 0.02723 | -0.02894 | -0.01452 | -0.00517 |

Table 4.18: Wavelet Coefficient Statistics at Various Levels for JPY/USD#4

| | d8 | d7 | d6 | d5 | d4 | d3 | d2 | d1 |
|---|---|---|---|---|---|---|---|---|
| mean | 0.00000 | -0.00003 | 0.00001 | -0.00001 | 0.00000 | -0.00001 | 0.00001 | -0.00000 |
| std | 0.00014 | 0.00014 | 0.00015 | 0.00014 | 0.00017 | 0.00021 | 0.00032 | 0.00047 |
| r(0) | 1.00000 | 1.00000 | 1.00000 | 1.00000 | 1.00000 | 1.00000 | 1.00000 | 1.00000 |
| r(1) | 0.01653 | -0.04560 | -0.08124 | 0.08312 | 0.05286 | 0.13461 | 0.20079 | 0.15060 |
| r(2) | 0.02851 | 0.06970 | -0.07742 | -0.02876 | -0.03634 | 0.00181 | -0.02653 | -0.02472 |
| r(3) | 0.18794 | 0.09722 | -0.12495 | -0.03817 | 0.05240 | 0.01047 | 0.00951 | 0.01681 |
| r(4) | 0.20890 | 0.02902 | 0.11354 | 0.02601 | -0.08626 | 0.01855 | 0.01937 | 0.00737 |

Table 4.19: Wavelet Coefficient Statistics at Various Levels for JPY/USD#5

| | d8 | d7 | d6 | d5 | d4 | d3 | d2 | d1 |
|---|---|---|---|---|---|---|---|---|
| mean | -0.00002 | 0.00000 | 0.00001 | -0.00001 | -0.00000 | 0.00000 | -0.00000 | 0.00000 |
| std | 0.00014 | 0.00014 | 0.00013 | 0.00014 | 0.00016 | 0.00021 | 0.00031 | 0.00043 |
| r(0) | 1.00000 | 1.00000 | 1.00000 | 1.00000 | 1.00000 | 1.00000 | 1.00000 | 1.00000 |
| r(1) | -0.16322 | 0.05817 | 0.01078 | -0.02612 | 0.08931 | 0.18613 | 0.17282 | 0.15362 |
| r(2) | 0.04007 | -0.08100 | -0.05011 | -0.02121 | -0.05463 | -0.04096 | -0.03782 | -0.03677 |
| r(3) | -0.06444 | 0.08629 | 0.01134 | -0.00423 | 0.02389 | 0.00577 | -0.00394 | 0.00572 |
| r(4) | -0.08300 | 0.05183 | -0.07329 | 0.03001 | 0.02105 | 0.02201 | 0.01143 | 0.02657 |

Table 4.20: Wavelet Coefficient Statistics at Various Levels for JPY/USD#6

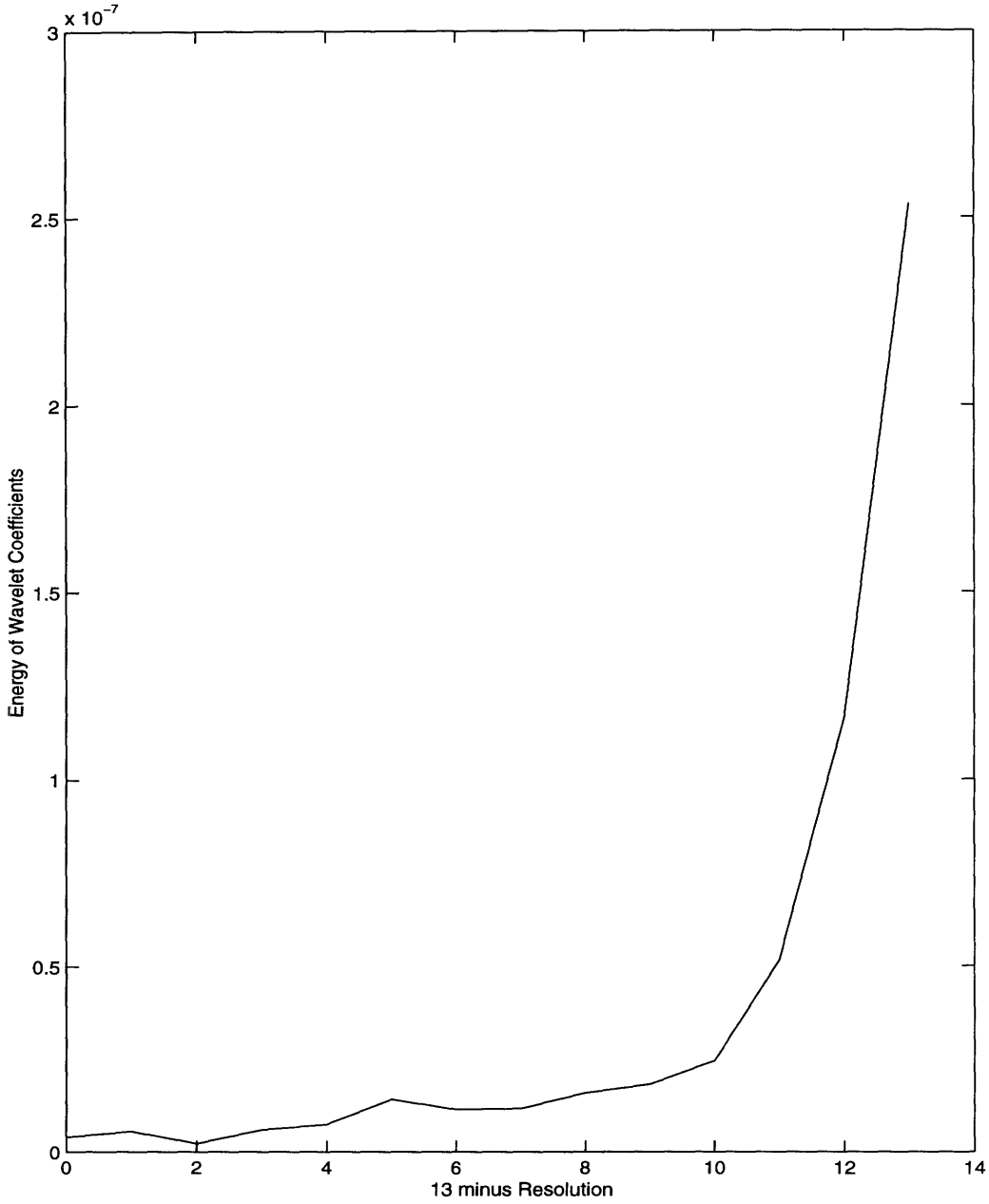


Figure 4-16: Wavelet Scalogram for JPY/USD#1

# Chapter 5

# Multiscale Modeling of Financial Data

## 5.1 The Data

The data used for parameter estimation of the the three multiresolution autoregressive models is the same as was used in Chapter 4. This means that we once again are dealing with returns on indices, individual stocks, and foreign exchange rates. The data is 8192 points long for the stocks and indices and 16384 long for the foreign exchange.

## 5.2 Results

The parameters of the 2- and 3-parameter autoregressive multiscale models were estimated using the minimum mean square error criternia described in Section 3.4. Tables 5.1 - 5.5 display the parameters.

| | $a_{\bar{\gamma}}$ | $b$ |
|---|---|---|
| CRSPEW | -0.02084 | 0.00845 |
| CRSPVW | -0.03214 | 0.00866 |
| SP500 | -0.03820 | 0.00870 |

| | $a_{\bar{\gamma}}$ | $b$ | $\lambda$ |
|---|---|---|---|
| CRSPEW | -0.02084 | 0.01234 | 0.08411 |
| CRSPVW | -0.03214 | 0.00946 | 0.01663 |
| SP500 | -0.03820 | 0.00942 | 0.01487 |

| | $a_1$ | $a_2$ | $b$ |
|---|---|---|---|
| CRSPEW | -0.02499 | -0.09785 | 0.00845 |
| CRSPVW | -0.03538 | -0.06457 | 0.00866 |
| SP500 | -0.04178 | -0.06403 | 0.00871 |

Table 5.1: Parameter Estimation for Indices
(a) 2-Parameter $AR(1)$, (b) 3-Parameter $AR(1)$ and (c) 3-Parameter $AR(2)$.

| | $a_{\bar{\gamma}}$ | $b$ |
|---|---|---|
| ALD | -0.05217 | 0.01769 |
| HPC | -0.01879 | 0.01663 |
| IBM | -0.04193 | 0.01426 |
| KO | -0.03952 | 0.01504 |
| MO | -0.01316 | 0.01569 |
| OAT | 0.01522 | 0.01720 |
| PW | -0.01080 | 0.01895 |
| TXN | 0.00645 | 0.02140 |
| UAL | 0.00430 | 0.02536 |
| XON | -0.05530 | 0.01249 |

Table 5.2: Parameter Estimation for 2-Parameter AR(1) Model for Stocks

| | $a_{\bar{\gamma}}$ | $b$ | $\lambda$ |
|---|---|---|---|
| ALD | -0.05217 | 0.01341 | -0.07578 |
| HPC | -0.01879 | 0.01560 | -0.02394 |
| IBM | -0.04193 | 0.01681 | 0.05334 |
| KO | -0.03952 | 0.01432 | -0.00785 |
| MO | -0.01316 | 0.01367 | -0.04323 |
| OAT | 0.01522 | 0.01531 | -0.02877 |
| PW | -0.01080 | 0.00826 | -0.17799 |
| TXN | 0.00645 | 0.02198 | -0.00048 |
| UAL | 0.00430 | 0.02457 | -0.01570 |
| XON | -0.05530 | 0.00783 | -0.12177 |

Table 5.3: Parameter Estimation for 3-Parameter AR(1) Model for Stocks

| | $a_1$ | $a_2$ | $b$ |
|---|---|---|---|
| ALD | -0.05246 | -0.02058 | 0.01771 |
| HPC | -0.02055 | -0.06929 | 0.01663 |
| IBM | -0.04259 | -0.02004 | 0.01427 |
| KO | -0.04011 | -0.02067 | 0.01505 |
| MO | -0.01312 | -0.03255 | 0.01569 |
| OAT | 0.01469 | -0.02309 | 0.01720 |
| PW | -0.01275 | 0.07606 | 0.01895 |
| TXN | 0.00614 | -0.01606 | 0.02140 |
| UAL | 0.00416 | -0.01023 | 0.02536 |
| XON | -0.05632 | -0.02434 | 0.01251 |

Table 5.4: Parameter Estimation for 3-Parameter AR(2) Model for Stocks

| | $a_{\bar{\gamma}}$ | $b$ |
|---|---|---|
| $JPY/USD_1$ | 0.01325 | 0.00041 |
| $JPY/USD_2$ | -0.10456 | 0.00037 |
| $JPY/USD_3$ | -0.18067 | 0.00036 |
| $JPY/USD_4$ | -0.07027 | 0.00038 |
| $JPY/USD_5$ | 0.00445 | 0.00038 |
| $JPY/USD_6$ | -0.01969 | 0.00035 |

| | $a_{\bar{\gamma}}$ | $b$ | $\lambda$ |
|---|---|---|---|
| $JPY/USD_1$ | 0.01325 | 0.00005 | -0.42482 |
| $JPY/USD_2$ | -0.10456 | 0.00003 | -0.48720 |
| $JPY/USD_3$ | -0.18067 | 0.00003 | -0.51983 |
| $JPY/USD_4$ | -0.07027 | 0.00008 | -0.27131 |
| $JPY/USD_5$ | 0.00445 | 0.00007 | -0.32663 |
| $JPY/USD_6$ | -0.01969 | 0.00008 | -0.27131 |

| | $a_1$ | $a_2$ | $b$ |
|---|---|---|---|
| $JPY/USD_1$ | 0.01114 | 0.18754 | 0.00041 |
| $JPY/USD_2$ | -0.09871 | 0.14505 | 0.00037 |
| $JPY/USD_3$ | -0.16114 | 0.16513 | 0.00036 |
| $JPY/USD_4$ | -0.07371 | 0.15573 | 0.00038 |
| $JPY/USD_5$ | -0.00240 | 0.15659 | 0.00038 |
| $JPY/USD_6$ | -0.02158 | 0.15433 | 0.00035 |

Table 5.5: Parameter Estimation for Foreign Exchange
(a) 2-Parameter $AR(1)$, (b) 3-Parameter $AR(1)$ and (c) 3-Parameter $AR(2)$.

From these tables we can calculate that the average $a$ for the AR(1) model for stocks is -.0206, which closely corresponds to the average $a$ for the equal-weighted index. It is appropriate to compare the the equal-weighted index because we have weighted the $a$'s equally. Furthermore, the average $a$'s for the AR(2) model for stocks are -.0213 and -.0161. This corresponds to less to that of the equal-weighted portfolio, however, it is closer to the parameters of CRSPEW than either of the other portfolios.

The results for the foreign exchange data shows that the data is nonstationary and must be modeled over small intervals. However, the really striking result from this data set is the high absolute value of $\lambda$ for the 3-parameter AR(1) model. This corresponds with the notion of self-similarity.

# Chapter 6

# Conclusion

## 6.1 Summary of Research

Multirate signal processing and the discrete wavelet transform, in particular, are described from both the analysis and synthesis viewpoint. The ability of the wavelet transform to decorrelate data and give a time-scale perspective will serve as an important tool in financial modeling. Factors such as QMF choice and finite-datalength effects are discussed.

Three multiresolution autoregressive models were described and the parameters were estimated for various individual stocks, stock indices and foreign exchange rates. The motivation behind using a multiresolution model stems from the fact that information and decisions are made by people and not made on any particular scale. By allowing the model to describe the behavior of the stock at different scales, we have described a robust modeling tool for financial time series. The use of these models are motivated by a multiresolution analysis of wavelet coefficient statistics at various scales.

The multiresolution analysis provide preliminary results that would suggest some practical use of encorporating wavelet and multiresolution techniques in the class of useful tools for analyzing financial time series.

The parameter estimates of the multiresolution models shows common behavior between several of the stocks and the indices. Furthermore, the results of the 2-

parameter AR(1) model estimates for foreign exchange returns suggests that this data might exhibit self-similarity.

While multiresolution seems to be an intuitive means of examining financial data, we do not have a good means of describing the parameters of our models in as intuitive a way.

## 6.2 Suggestions for Future Research

Future research needs to be done to both explain the practical meaning of the parameters of multiresolution models, and relate the behavior of these parameters to company size, sector, etc. It would also be of interest to use some notion of similarity between two processes in a statistical sense, e.g., Bhattacharyya distance, to create a means of determining when one should use different order autoregressive models. The idea of stationarity as introduced by Basseville, et al. [6], also appeals in this sense, as one can use normal time series approaches to determining model order, i.e., partial autocorrelation (PARCOR) or reflection coefficients.

Another interesting field of study would be investigating the apparent indications of self-similar behavior in the foreign exchange data. The model parameters, especially in models that use scale-varying variance for the driving white-noise, could prove to be optimal in an information bearing sense. This statement is motivated by the idea that self-similarity represents a phenomenon that is not based in one scale, but rather at all scales. By using the scale-varying model parameter $\lambda$, we could focus only on the behavior that is scale-invariant.

A final note should be made that this study has been conducted as a first step to initialize the notion of multiresolution with the reader. The results are of a very general nature and a more detailed study should be conducted to further explain the model parameters. Finally, more study on the class of signals that can be derived using our multiscale models and the relation of these time series models to asset pricing should be conducted.

# Appendix A

# Frequency Histograms of Wavelet Coefficients

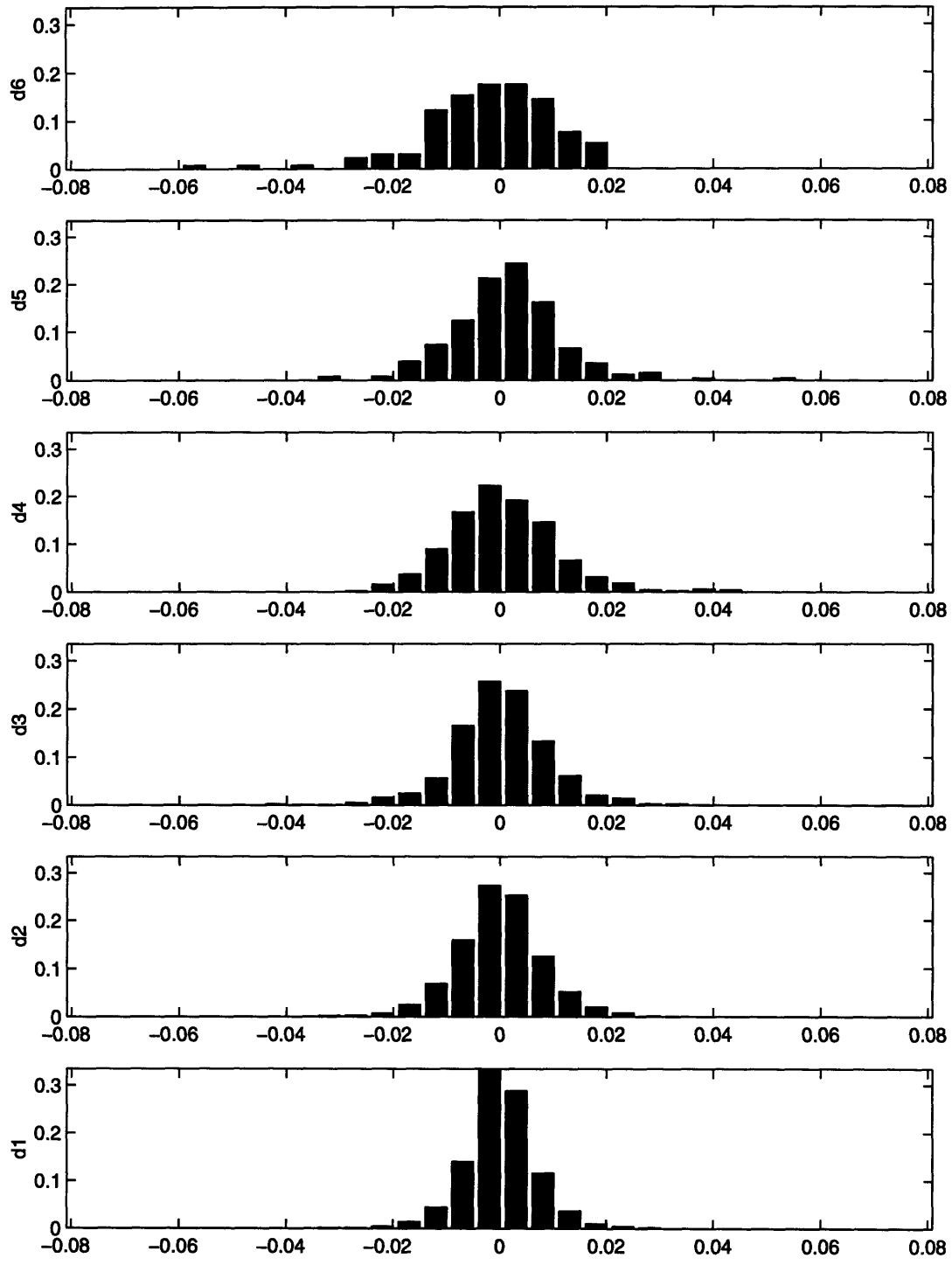


Figure A-1: Frequency Histograms of Wavelet Coefficients for CRSPEW

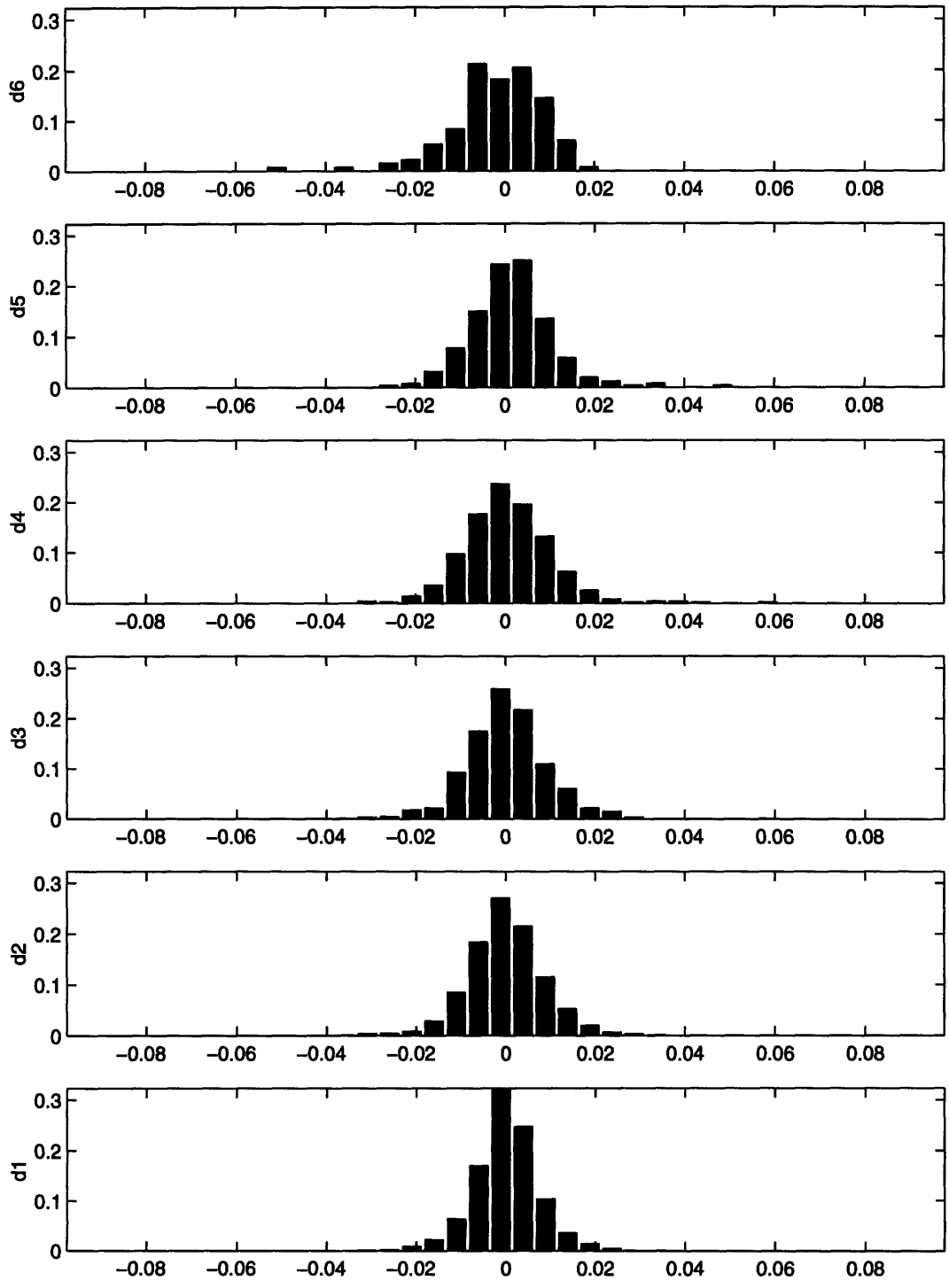


Figure A-2: Frequency Histograms of Wavelet Coefficients for CRSPVW

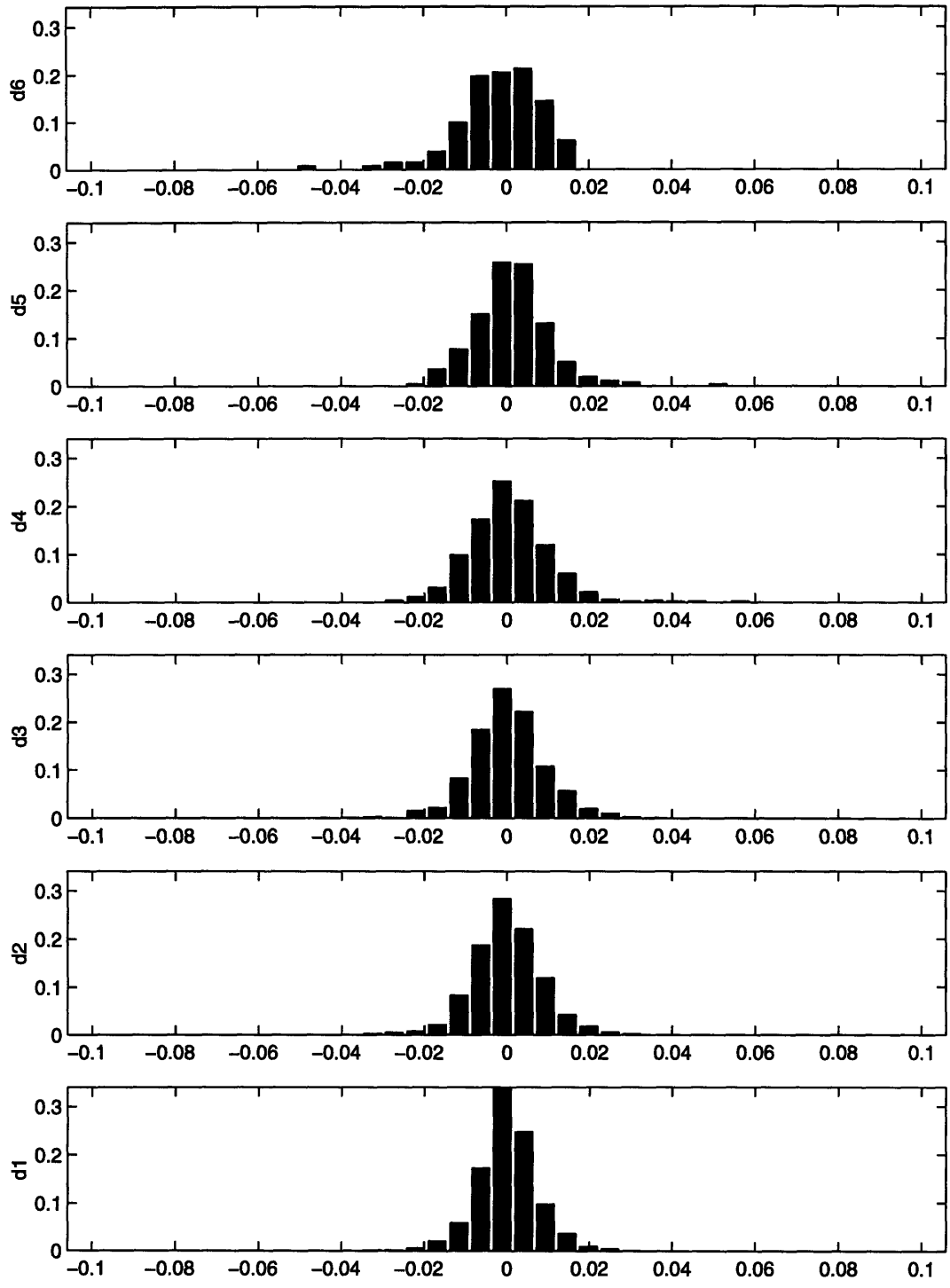


Figure A-3: Frequency Histograms of Wavelet Coefficients for SP500

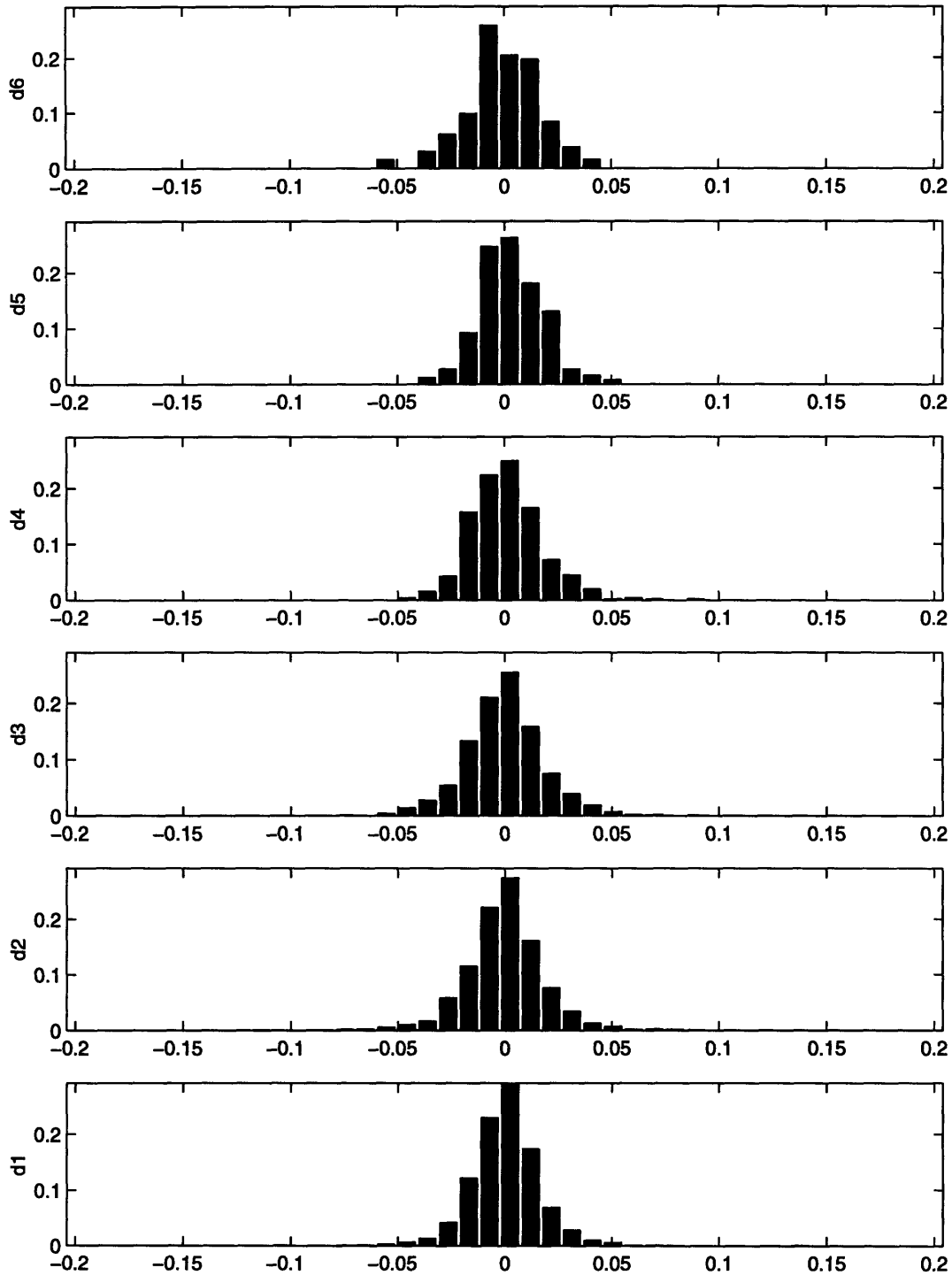


Figure A-4: Frequency Histograms of Wavelet Coefficients for ALD

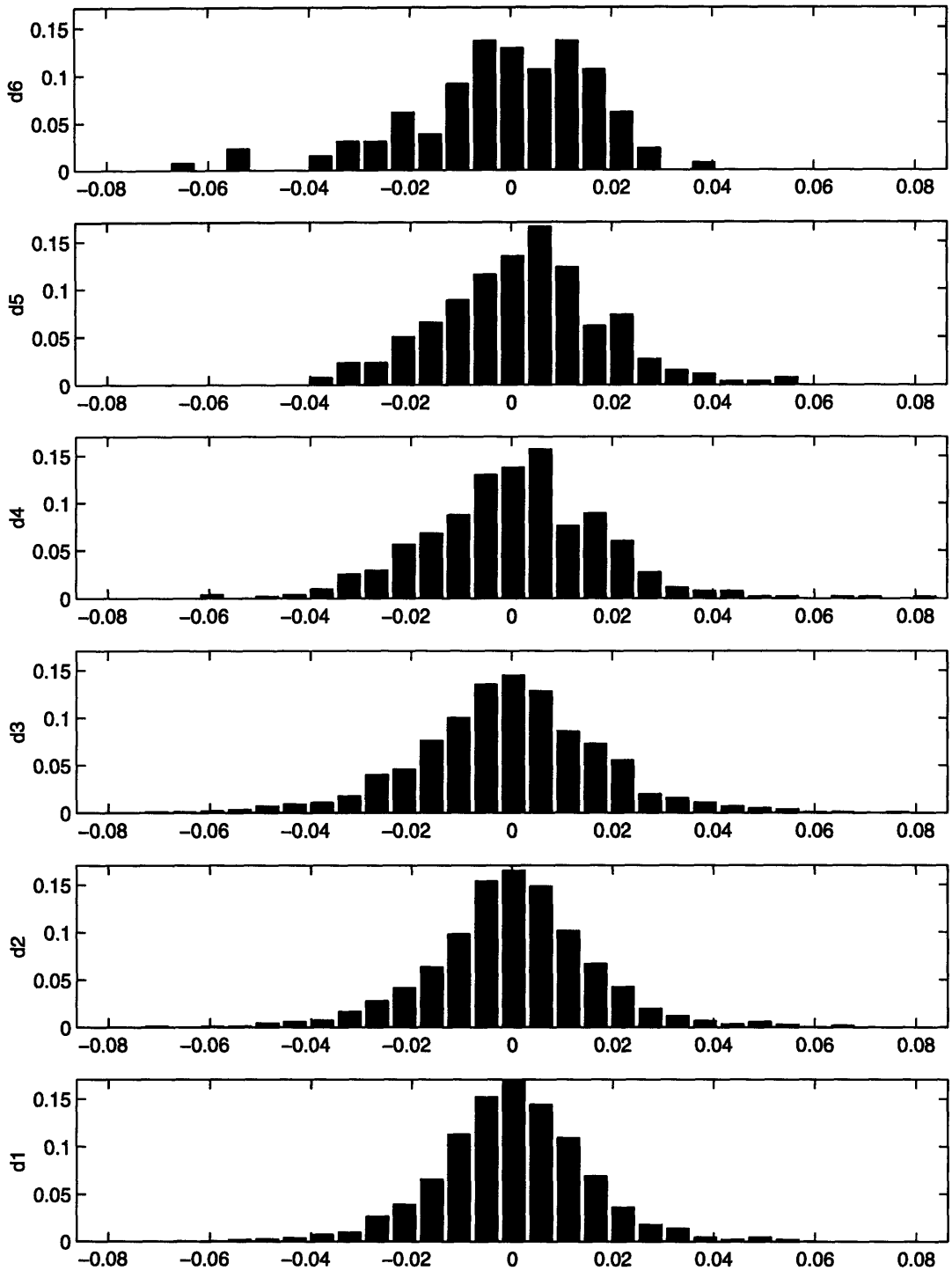


Figure A-5: Frequency Histograms of Wavelet Coefficients for HPC

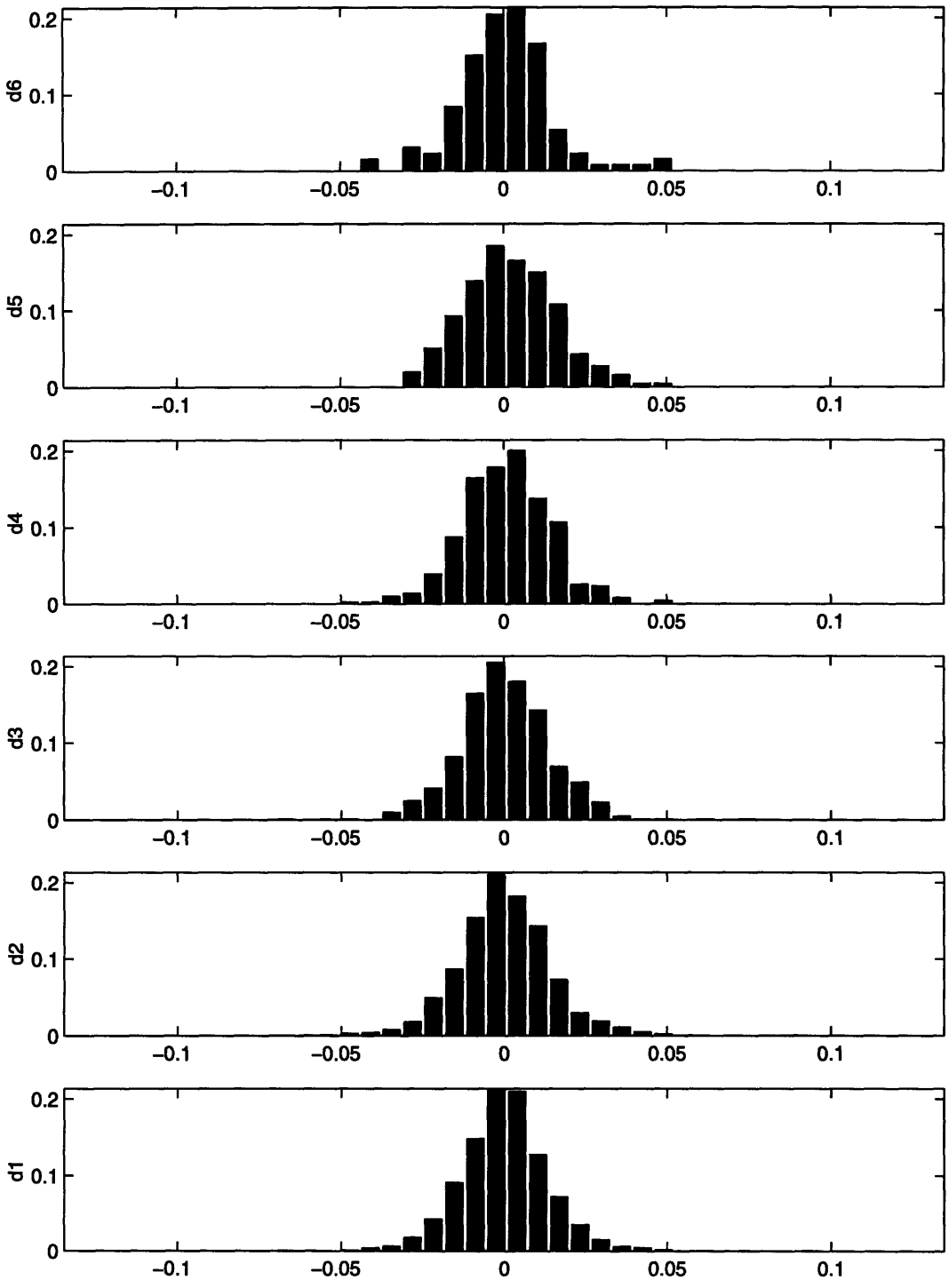


Figure A-6: Frequency Histograms of Wavelet Coefficients for IBM

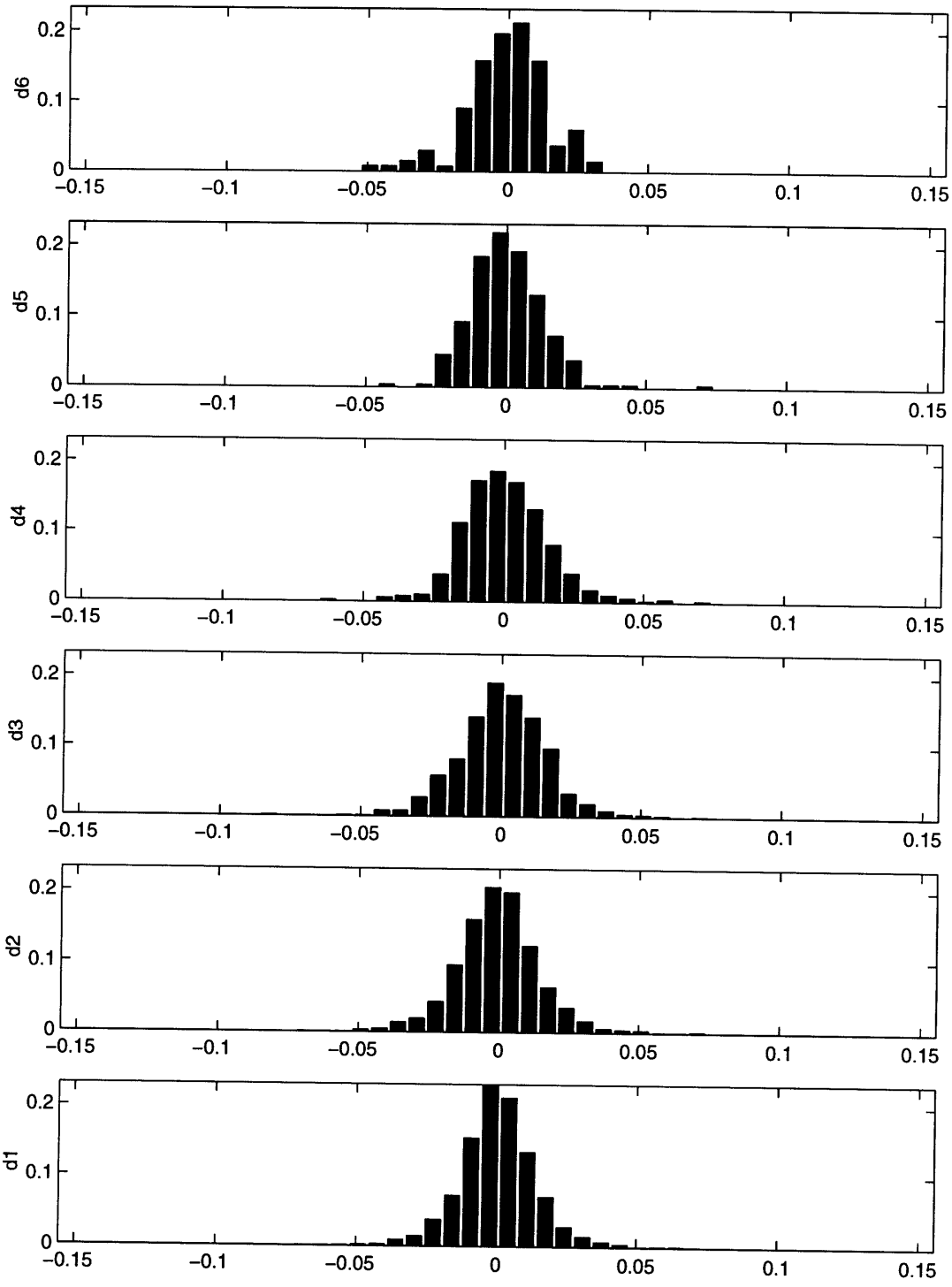


Figure A-7: Frequency Histograms of Wavelet Coefficients for KO

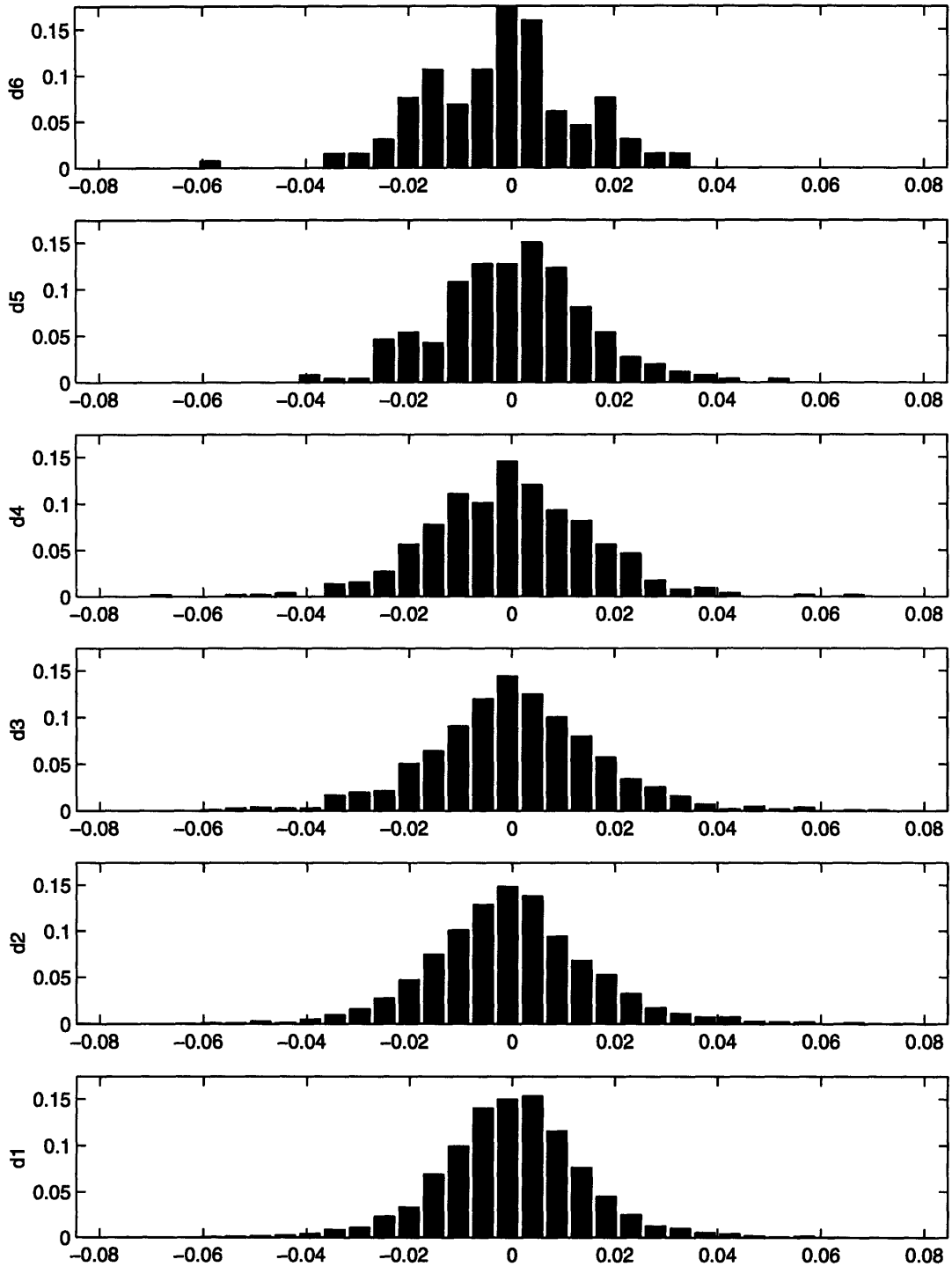


Figure A-8: Frequency Histograms of Wavelet Coefficients for MO

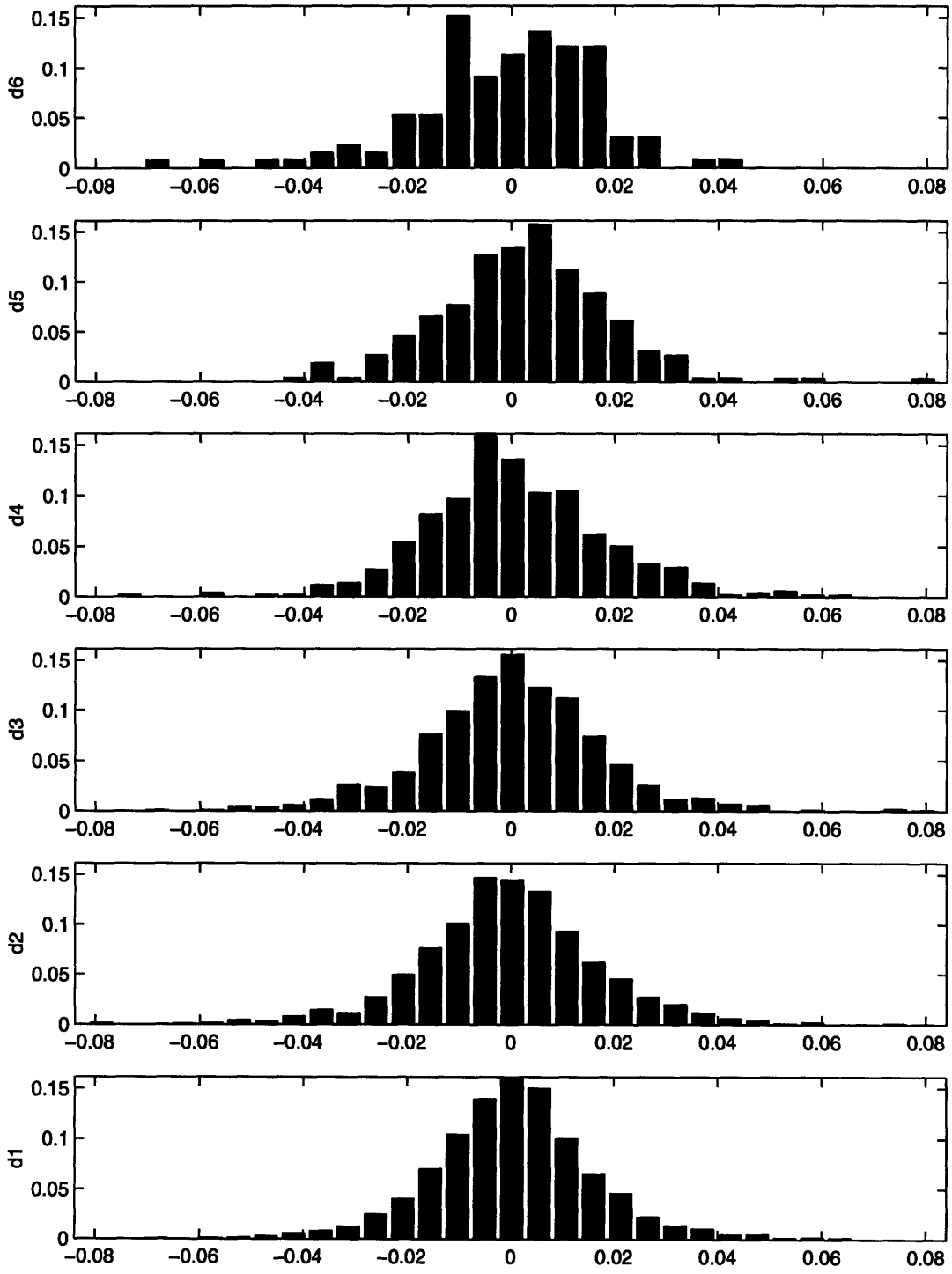


Figure A-9: Frequency Histograms of Wavelet Coefficients for OAT

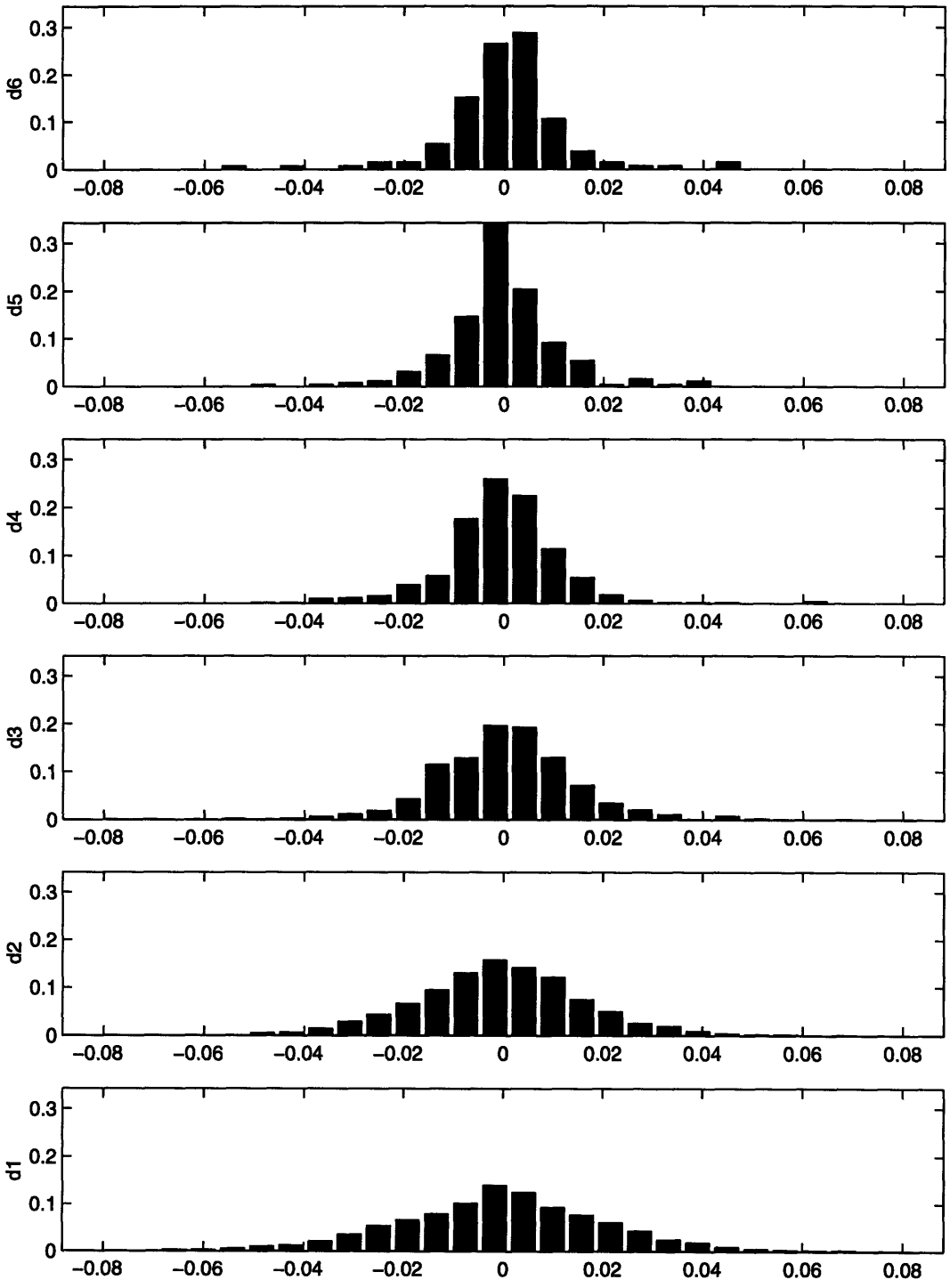


Figure A-10: Frequency Histograms of Wavelet Coefficients for PW

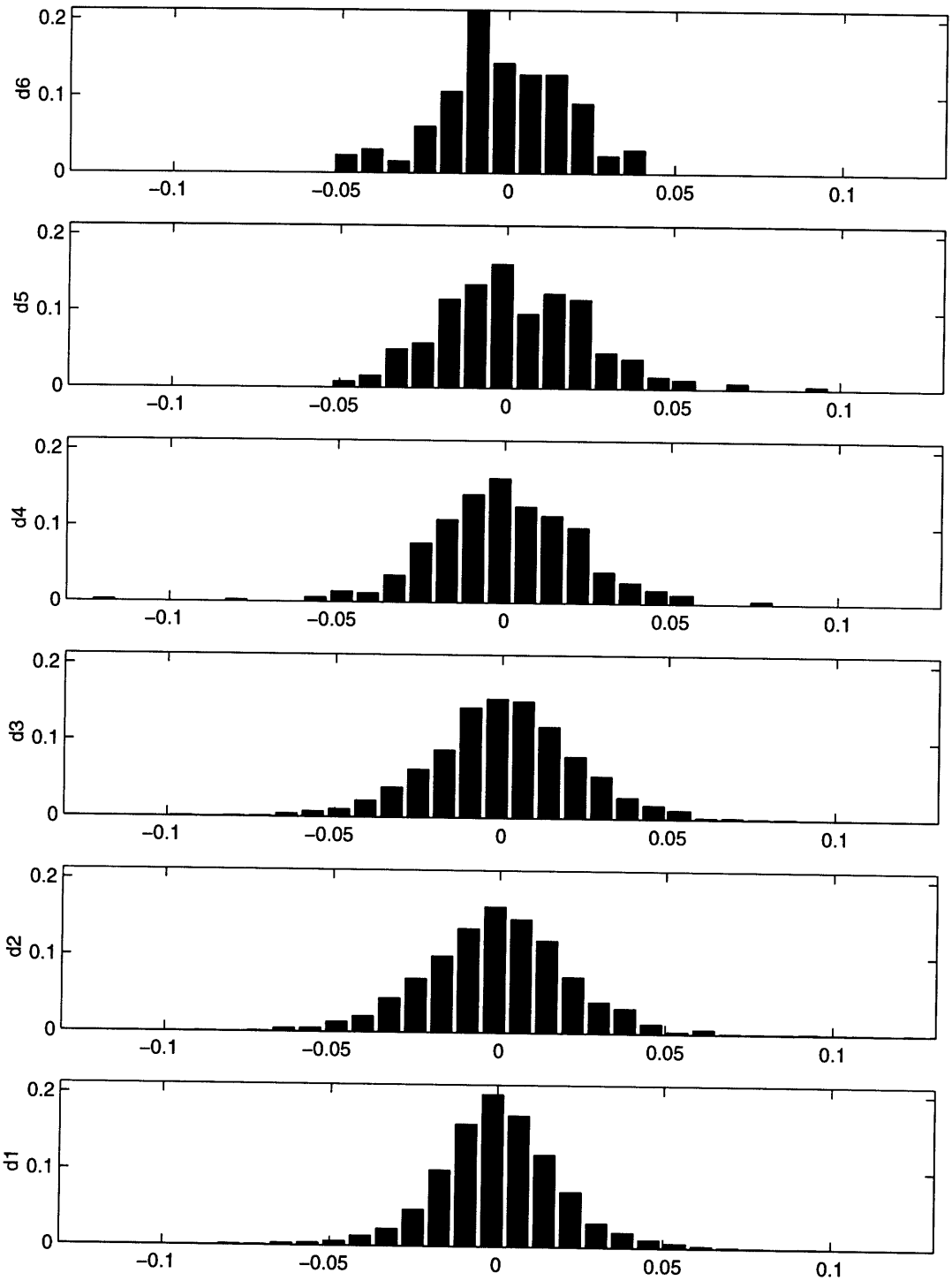


Figure A-11: Frequency Histograms of Wavelet Coefficients for TXN

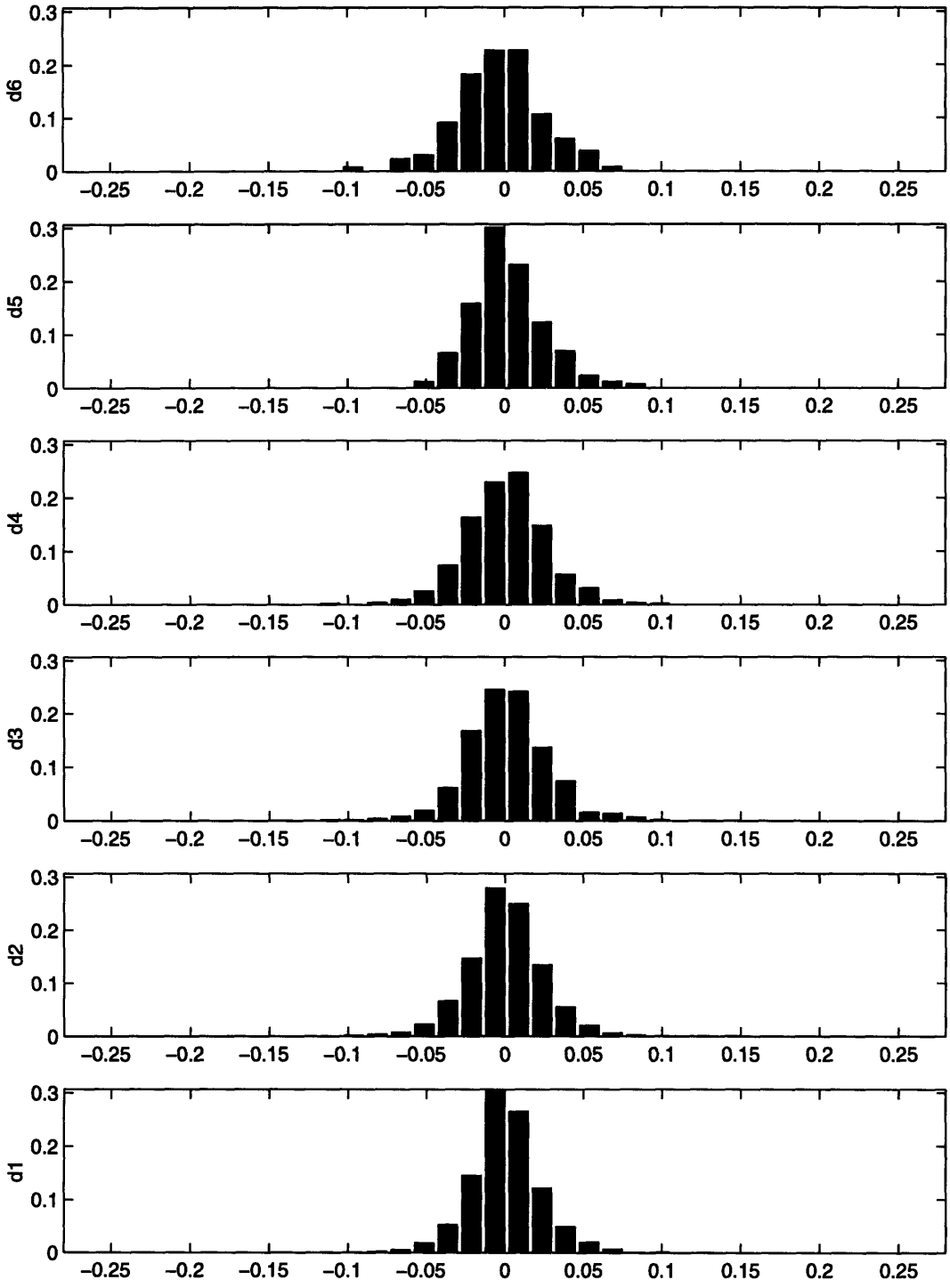


Figure A-12: Frequency Histograms of Wavelet Coefficients for UAL

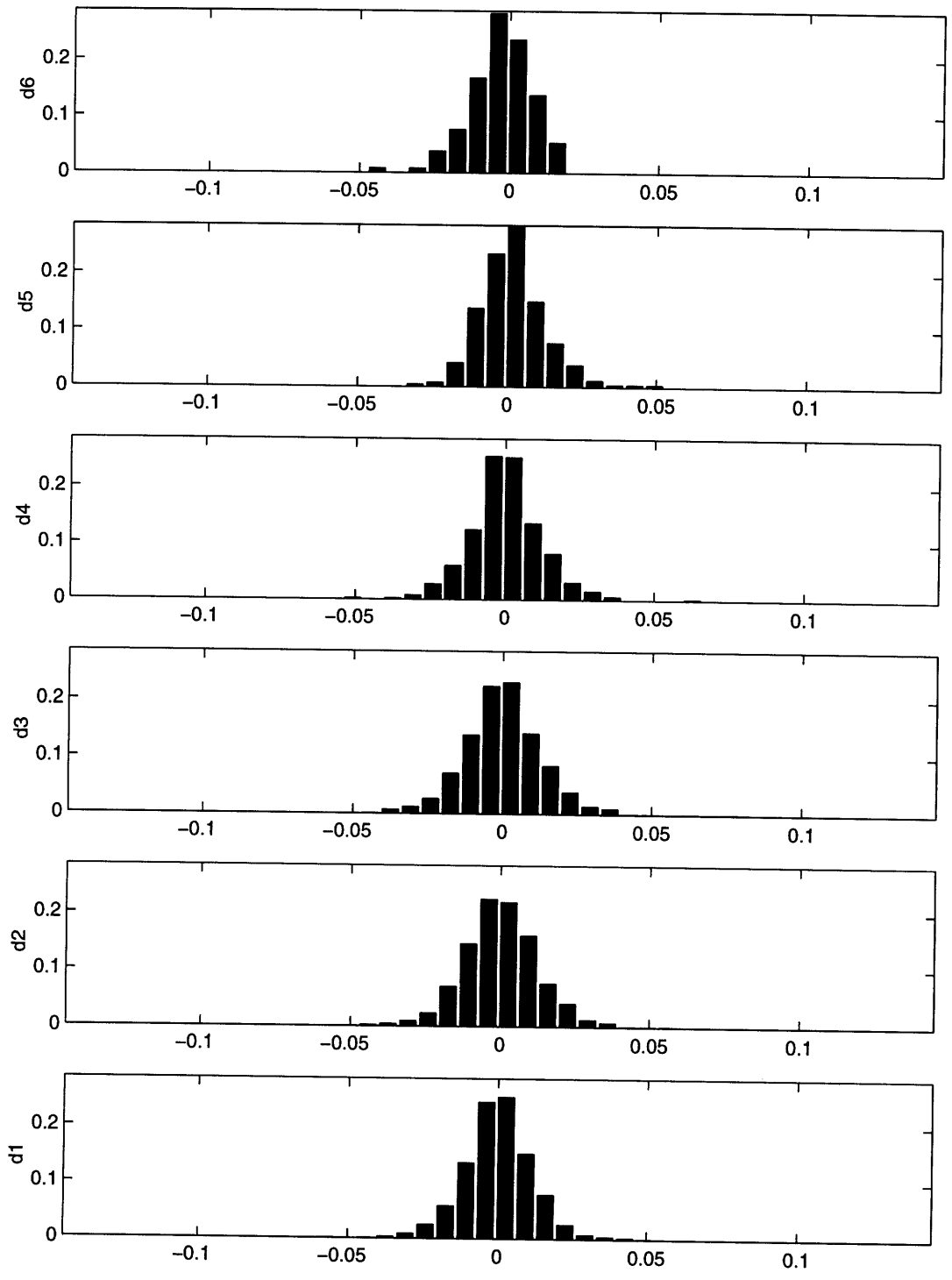


Figure A-13: Frequency Histograms of Wavelet Coefficients for XON

# Appendix B

# Wavelet Coefficient Intensity Plots

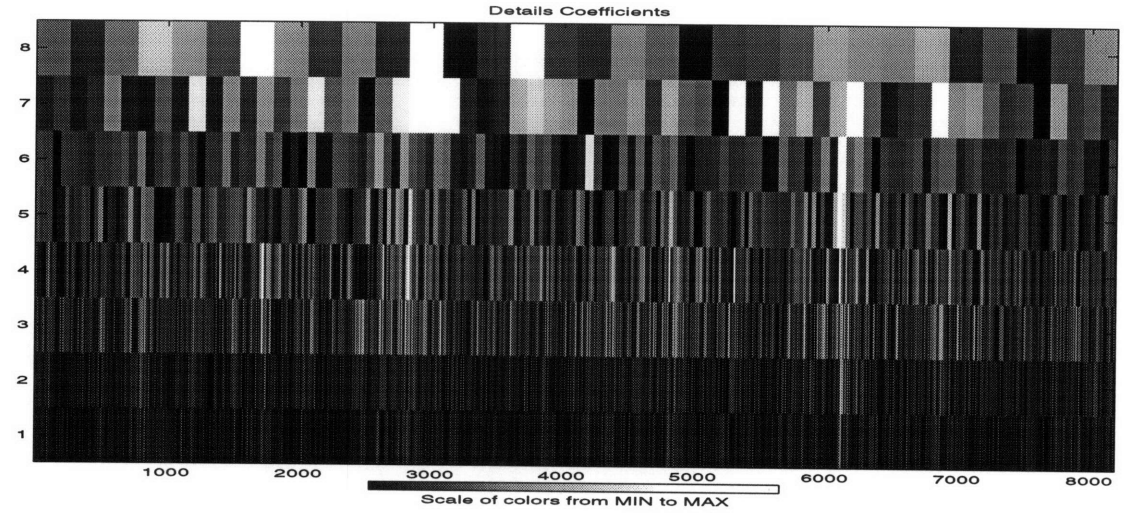


Figure B-1: Wavelet Coefficient Intensity by Dilation and Translation for CRSPVW

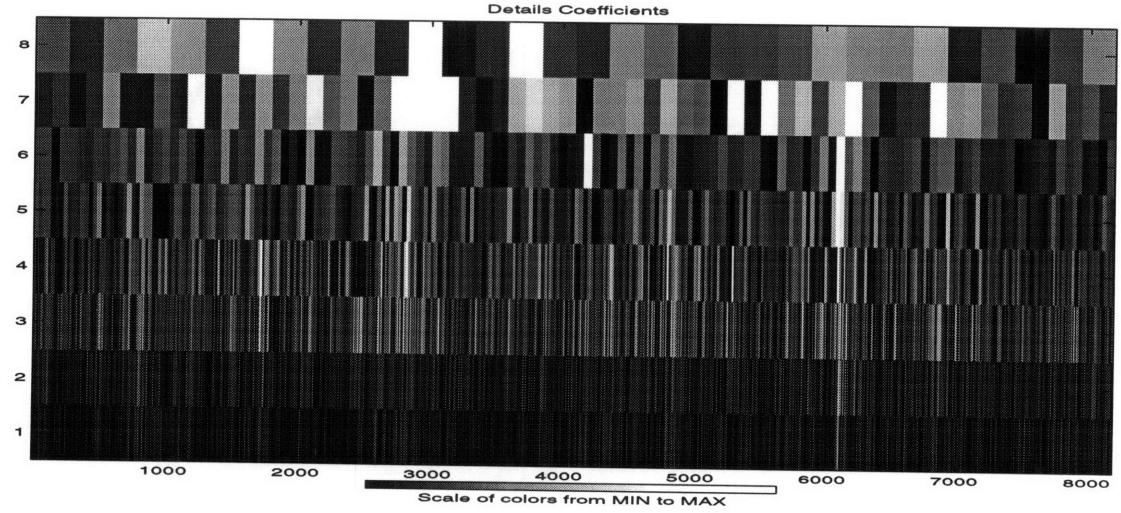


Figure B-2: Wavelet Coefficient Intensity by Dilation and Translation for SP500

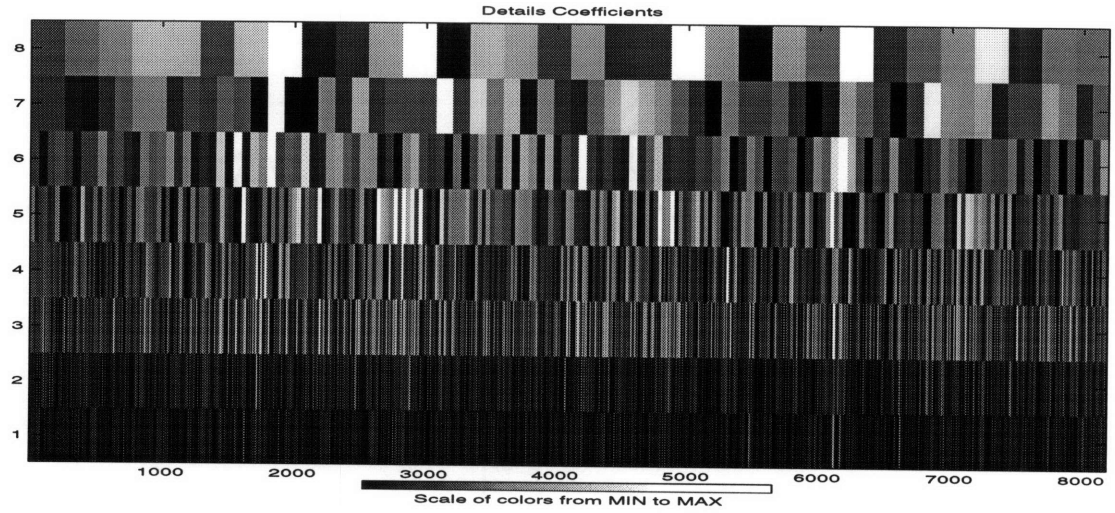


Figure B-3: Wavelet Coefficient Intensity by Dilation and Translation for ALD

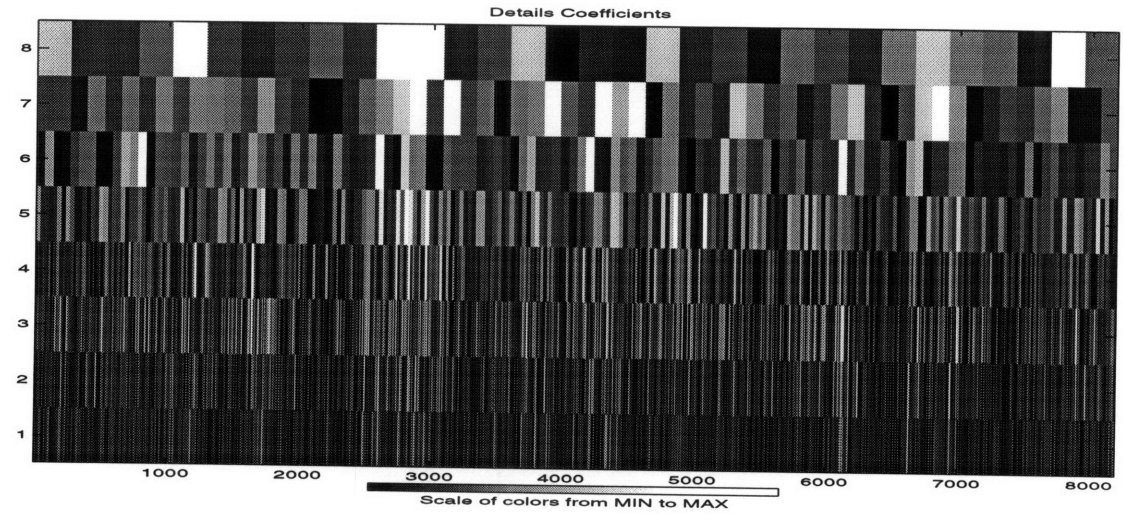


Figure B-4: Wavelet Coefficient Intensity by Dilation and Translation for HPC

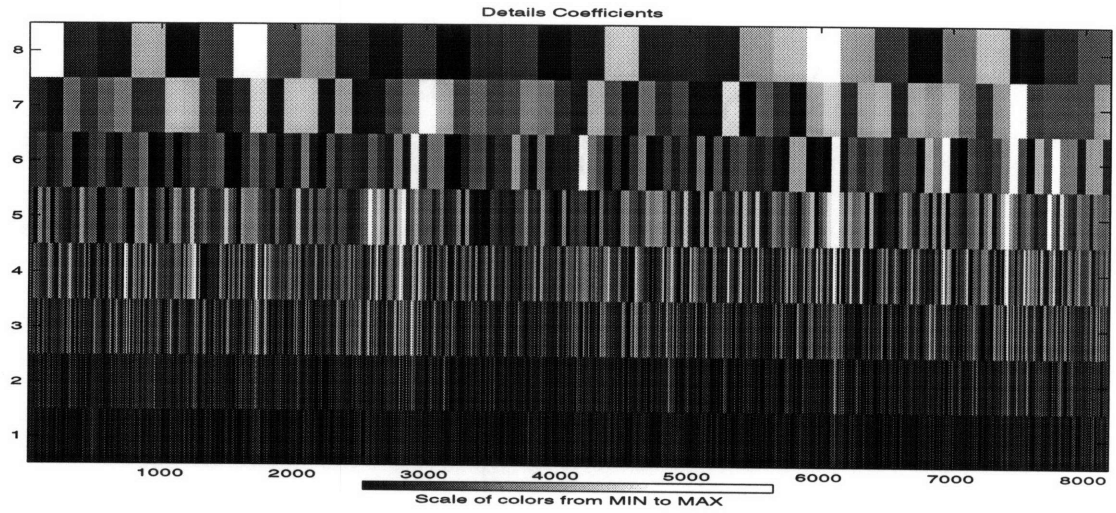


Figure B-5: Wavelet Coefficient Intensity by Dilation and Translation for IBM

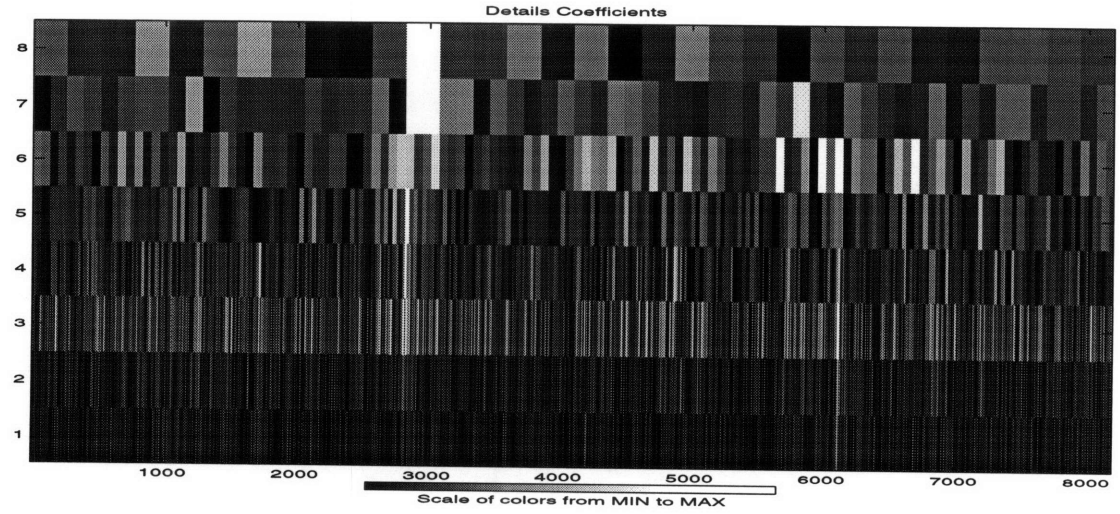


Figure B-6: Wavelet Coefficient Intensity by Dilation and Translation for KO

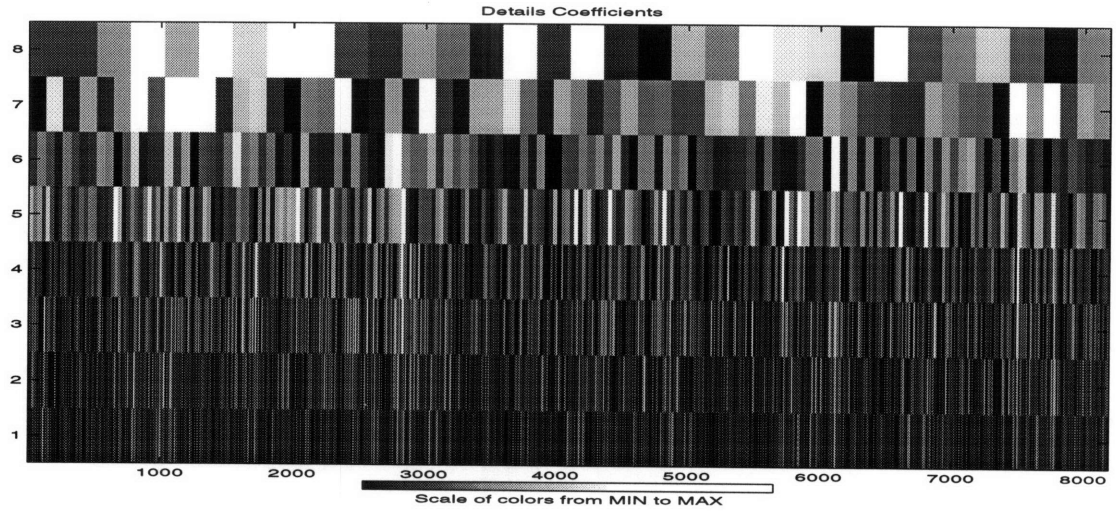


Figure B-7: Wavelet Coefficient Intensity by Dilation and Translation for MO

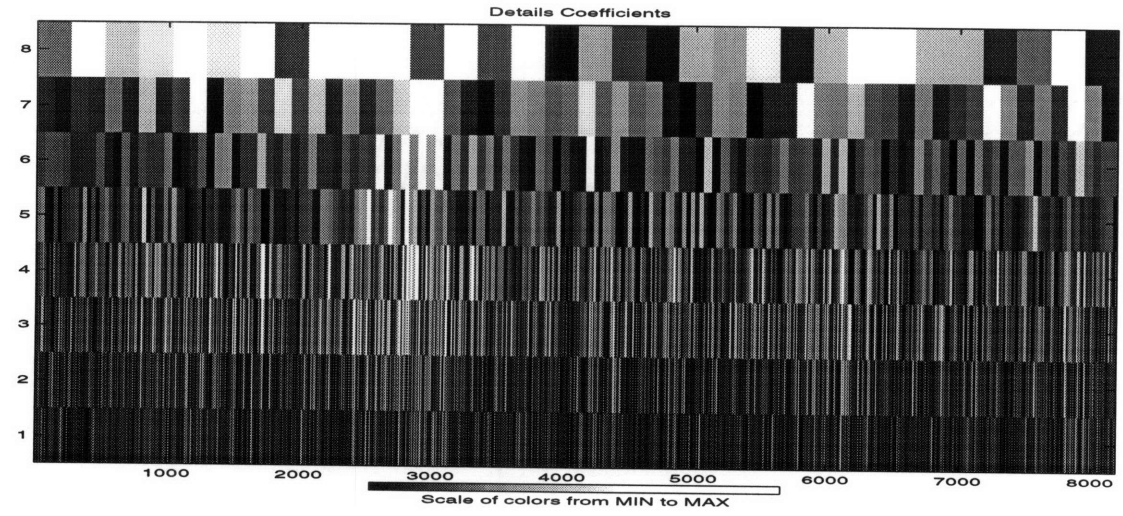


Figure B-8: Wavelet Coefficient Intensity by Dilation and Translation for OAT

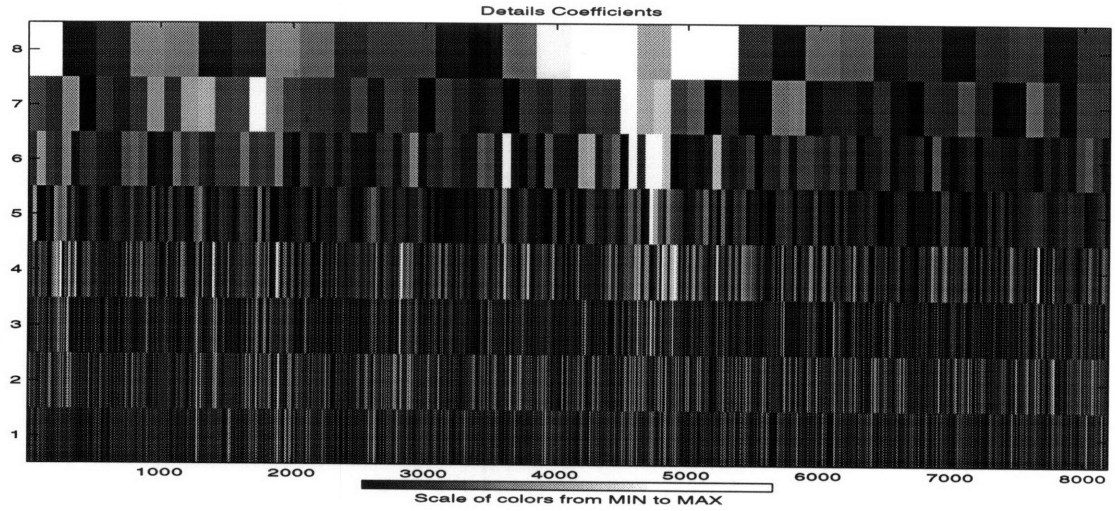


Figure B-9: Wavelet Coefficient Intensity by Dilation and Translation for PW

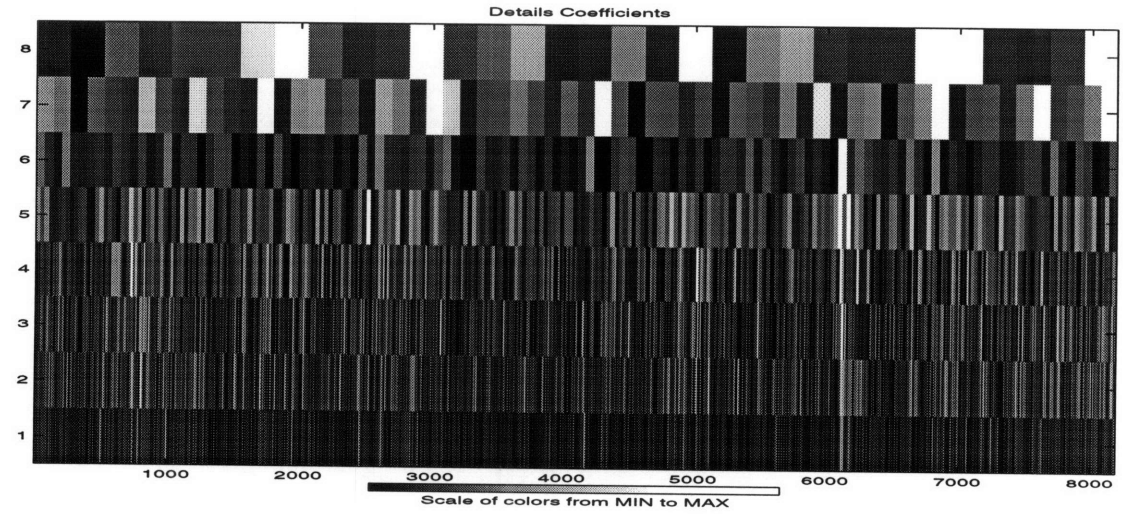


Figure B-10: Wavelet Coefficient Intensity by Dilation and Translation for TXN

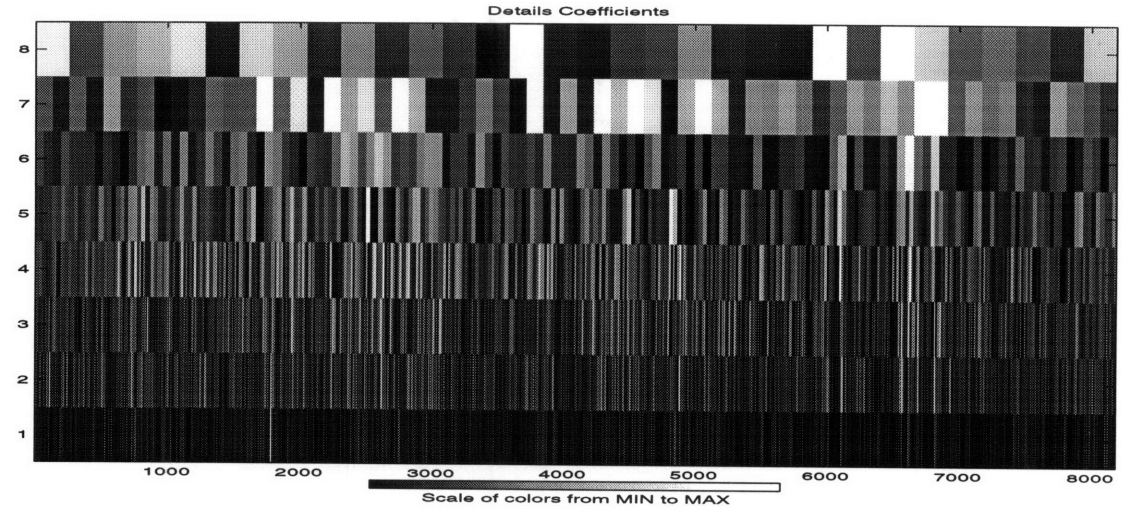


Figure B-11: Wavelet Coefficient Intensity by Dilation and Translation for UAL

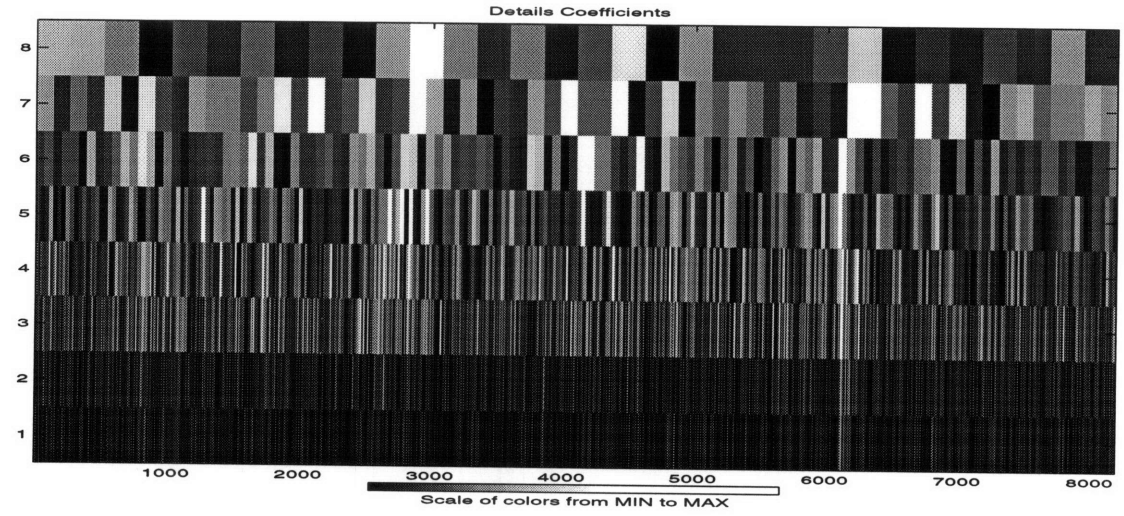


Figure B-12: Wavelet Coefficient Intensity by Dilation and Translation for XON

# Bibliography


[1] Patrice Abry, Paulo Gonçalvès, and Patrick Flandrin. Wavelets, spectrum analysis and $1/f$ processes. In Anestis Antoniadis and Georges Oppenheim, editors, *Wavelets and Statistics*, volume 103 of *Lecture Notes in Statistics*. Springer-Verlag, 1995.

[2] A.N. Akansu and R.A. Haddad. *Multiresolution Signal Decomposition*. Academic Press, 1992.

[3] Miguel A. Arino. Time series forecasts via wavelets: an application to car sales in the spanish market. Technical report, Duke University: Institute of Statistics and Decision Sciences, 1995.

[4] Miguel A. Arino and Brani Vidakovic. On wavelet scalograms and their applications in economic time series. Technical report, Duke University: Institute of Statistics and Decision Sciences, 1995.

[5] A. Arnedo et al. Characterizing long-range correlations in dna sequences from wavelet analysis. *Physical Review Letters*, 74(16), 1995.

[6] M. Basseville et al. Modeling and estimation of multiresolution stochasic processes. *IEEE Transactions on Information Theory*, 38, 1992.

[7] Edward W. Bolton, Kirk A. Maasch, and Jonathan M. Lilly. A wavelet analysis of plio-pleistocene climate indicators: A new view of periodicity evolution. *Geophysical Research Letters*, 22(20), 1995.

[8] P.J. Burt and E.H. Adelson. The laplacian pyramid as a a compact image code. *IEEE Transactions on Communications*, COM-31, 1983.

[9] K. Chou et al. Multiresolution stochastic models, data fusion, and wavelet transforms. *Signal Processing*, 34, 1993.

[10] Kenneth C. Chou. *A Stochastic Modeling Approach to Multiscale Signal Processing.* PhD Thesis, MIT, 1991.

[11] A. Cohen and R.D. Ryan. *Wavelets and Multiscale Signal Processing.* Chapman and Hall, 1995.

[12] R.E. Croshiere and L.R. Rabiner. *Multirate Digital Signal Processing.* Prentice Hall, 1983.

[13] I. Daubechies. Orthonormal bases of compactly supported wavelets. *Communications in Pure Applied Mathematics*, 41, 1988.

[14] I. Daubechies. *Ten Lectures on Wavelets.* SIAM, 1992.

[15] Anthony Davis, Alexander Marshak, and Warren Wiscombe. Wavelet-based multifractal analysis of non-stationary and/or intermittent geophysical signals. In Efi Foufoula-Georgiou and Praveen Kumar, editors, *Wavelets in Geophysics*, volume 4 of *Wavelet Analysis and Its Applications.* Academic Press, 1994.

[16] Robert Dijkerman and Ravi Mazumdar. On the correlation structure of the wavelet coefficients of fractional brownian motion. *IEEE Transactions on Information Theory*, 40, 1994.

[17] Robert Dijkerman and Ravi Mazumdar. Wavelet representations of stochastic processes and multiresolution stochastic models. *IEEE Transactions on Signal Processing*, 42, 1994.

[18] D.L. Donoho. *Interpolating Wavelet Transforms.* Department of Statistics, Stanford University, Stanford, CA, 1992.

[19] N.J. Fliege. *Multirate Digital Signal Processing.* John Wiley, 1994.

[20] Stuart A. Golden. *Identifying Multiscale Statistical Models using the Wavelet Transform.* MIT E.E. and S.M. Thesis, 1991.

[21] P. Goupillaud, A. Grossmann, and J. Morlet. Cycle-octave and related transforms in seismic signal analysis. *Geoexploration*, 23, 1985.

[22] Amara Graps. An introduction to wavelets. *IEEE Computational Science and Engineering*, 2, 1995.

[23] Alfred Haar. Zur theorie der orthogonalen funktionen-systeme. *Math. Ann.*, 69, 1910.

[24] C. L. Jones, G. T. Lonergan, and D. E. Mainwaring. Wavelet packet computation of the hurst exponent. *Journal of Physics A: Mathematical and General*, 29(10), 1996.

[25] Lance M. Kaplan and C.-C. Jay Kuo. Extending self-similarity for fractional brownian motion. *The Annals of Statistics*, 24(12), 1996.

[26] Ronald W. Lindsay, Donald B. Percival, and D. Andrew Rothrock. The discrete wavelet transform and the scale analysis of the surface properties of sea ice. *IEEE Transactions on Geoscience and Remote Sensing*, 34(3), 1996.

[27] S. Mallat. *Wavelet Signal Processing.* Academic Press, 1996.

[28] Stephane Mallat. *Multiresolution Representations and Wavelets.* PhD Thesis, University of Pennsylvania, 1988.

[29] Stephane Mallat. Multiresolution approximations and wavelet orthonormal bases of $l^2(r)$. *Transactions of the American Mathematical Society*, 315, 1989.

[30] Yves Meyer. *Wavelets and Operators.* Cambridge University Press, 1993.

[31] Frédérique Moreau, Dominique Gilbert, and Ginette Saracco. Filtering non-stationary geophysical data with orthogonal wavelets. *Geophysical Research Letters*, 23(4), 1996.

[32] Donald B. Percival and Peter Guttorp. Long-memory processes, the allan variance and wavelets. In Efi Foufoula-Georgiou and Praveen Kumar, editors, *Wavelets in Geophysics*, volume 4 of *Wavelet Analysis and Its Applications*. Academic Press, 1994.

[33] James B. Ramsey, Daniel Usikov, and George M. Zaslavsky. An analysis of u.s. stock price behavior using wavelets. Technical report, New York University, 1994.

[34] T. Subba Rao and K.C. Indukumar. Spectral and wavelet methods for the analysis of nonlinear and nonstationary time series. *Journal of the Franklin Institute*, 333(3), 1996.

[35] O. Rioul and P. Duhamel. Fast algorithms for discrete and continuous wavelet transforms. *IEEE Transactions on Information Theory*, 1992.

[36] Gilbert Strang and Truong Nguyen. *Wavelets and Filter Banks*. Wellesley-Cambridge Press, Wellesley, MA, 1996.

[37] P.P. Vaidyanathan. Theory and design of m-channel maximally decimated quadrature mirror filters with arbitrary m, having the perfect reconstruction property. *IEEE Transactions on Acoustic and Speech Signal Processing*, 35, 1987.

[38] Gregory W. Wornell. Wavelet-based representations for the $1/f$ family of fractal processes. *Proceedings of the IEEE*, 81, 1993.

[39] Gregory W. Wornell. *Signal Processing with Fractals: A Wavelet-Based Approach*. Prentice Hall, Upper Saddle River, NJ, 1996.